

# **EXPERIMENTAL INVESTIGATION OF A COMBI BOILER HEAT EXCHANGER**

**A Thesis Submitted to  
the Graduate School of Engineering and Sciences of  
İzmir Institute of Technology  
in Partial Fulfillment of the Requirements for the Degree of**

**MASTER OF SCIENCE**


**in Mechanical Engineering**

**by  
Mehmet KARA**

**July, 2018  
İZMİR**

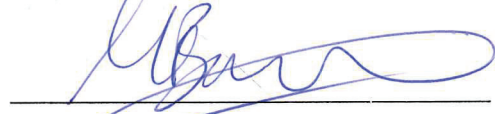
We approve thesis of **Mehmet KARA**

**Examining Committee Members:**



**Assoc. Prof. Dr. Erdal ÇETKİN**

Department of Mechanical Engineering, İzmir Institute of Technology.



**Dr. Murat BARIŞIK**

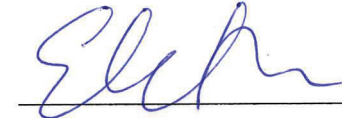
Department of Mechanical Engineering, İzmir Institute of Technology.



**Prof. Dr. Aytunç EREK**

Department of Mechanical Engineering, Dokuz Eylul University.

**09 July 2018**



**Assoc. Prof. Dr. Erdal ÇETKİN**

Supervisor, Department of  
Mechanical Engineering İzmir  
Institute of Technology

**Prof. Dr. Metin TANOĞLU**

Head of the Department of Mechanical  
Engineering

**Prof. Dr. Aysun SOFUEOĞLU**

Dean of the Graduate School  
of Engineering and Sciences

## **ACKNOWLEDGMENTS**

First of all, I would like to extend my gratitude to Erdal Çetkin for his guidance and endless support.

I am deeply grateful to Servet Yıldırım for helping me to choose this subject. He also shared with me his vast knowledge on this subject, guiding me, and provide motivation and support during the creation of the thesis.

I would like to thank Bosch Thermotechnology Manisa Company for giving the opportunity to work on my thesis.

And I am giving thanks to my friends and my family, especially to my mother Gülseren KARA, who always take my side and make me feel their support while completing my thesis.

# **ABSTRACT**

## **EXPERIMENTAL INVESTIGATION OF A COMBI BOILER HEAT EXCHANGER**

The combi boilers are divided into two types, condensing and conventional, in terms of waste gas heat recovery. In conventional types, the condensation occurrence is undesirable, and over time it causes corrosion in the main heat exchangers, which decrease the efficiency and the lifetime. Although life tests are performed to check if the condensation has occurred or not over time, these tests take a long time and require the high cost. In this thesis, it is aimed to find a heat transfer correlation and use the calculation method instead of life tests.

Two different topics were investigated on three appliances with different design parameters in order to find out in which conditions the condensation on the heat exchangers has occurred. As the first topic, influences of the fresh air amount in combustion equations, on condensation was tested in conventional appliances of Type B and C. As the second subject, the effects of the exchanger design parameters on the condensation were tested by using copper finned and stainless steel finned heat exchangers. For this study, mapping tests were carried out in the laboratories of Bosch Thermotechnology in Manisa and the measurement results of CO<sub>2</sub> percentages and temperature distributions of the combustion over the exchanger were used.

Using mapping test data, different condensation temperatures were calculated for three appliances depending on the fresh air amount and exchanger design parameters. These variables are able to be used in the heat transfer correlation to make improvements on the condensation point without making life tests.



# ÖZET

## BİR KOMBİ ISI DEĞİŞTİRGEÇİNİN DENEYSEL OLARAK İNCELENMESİ

Kombiler atık gaz ısısı geri kazanımı açısından yoğuşmalı ve konvansiyonel olmak üzere ikiye ayrılır. Konvansiyonel tip kombi cihazlarında yoğuşma istenmeyen bir durumdur ve zaman içinde bu yoğuşma oluşumu, cihazların ana ısı değiştirgecinde korozyona sebep olarak cihazın veriminin düşmesine ve cihazın ömrünün azalmasına sebep olur. Ömür testleri yapılarak zaman içerisinde korozyon oluşumu olup olmadığı kontrol edilmesine rağmen bu testler uzun zaman almakta ve yüksek maliyet gerektirmektedir. Bu tezde bir ısı transfer korelasyonu bulunarak ömür testleri yerine hesaplama yönteminin kullanılması amaçlanmıştır.

Isı değiştirgecinde yoğuşmanın hangi şartlarda meydana geldiğini anlamak için farklı tasarım parametrelerine sahip üç cihaz üzerinde iki farklı konu araştırılmıştır. İlk konu olarak, yanma denklemlerindeki taze hava miktarının yoğuşma üzerindeki etkileri, B ve C tipi geleneksel cihazlarda test edilmiştir. İkinci konu olarak, eşanjör tasarım parametrelerinin yoğuşma üzerindeki etkileri, bakır finli ve paslanmaz çelik finli ısı değiştirgeçleri kullanılarak test edilmiştir. Bu çalışma için Manisa'daki Bosch Termoteknik laboratuvarlarında haritalama testleri gerçekleştirilmiş ve ısı değiştirgeci üzerindeki, yanma sonucu oluşan CO<sub>2</sub> yüzdeleri ve sıcaklık dağılımlarının ölçüm sonuçları kullanılmıştır.

Haritalama test verileri kullanılarak yapılan hesaplamalar sonucunda hava miktarı ve tasarım parametrelerine bağlı olarak farklı yoğuşma sıcaklıkları bulunmuştur. Bu değişkenler bulunan korelasyon içinde kullanılarak test yapmaksızın yoğuşma noktası üzerinde iyileştirmeler yapmaya olanak sağlar.

# TABLE OF CONTENTS

LIST OF FIGURES .....	viii
LIST OF TABLES .....	xi
LIST OF SYMBOL.....	xiv
CHAPTER 1. INTRODUCTION.....	1
1.1. Combi Boiler.....	1
1.1.1. Categorized of the Combi Boilers.....	2
1.1.1.1. Type A .....	3
1.1.1.2. Type B – Open Flue (OF) Appliance .....	3
1.1.1.3. Type C – Room Sealed Flue (RSF) Appliance.....	4
1.1.2. The Components of the Combi Boilers.....	7
1.2. Heat Exchangers (HEX).....	11
1.2.1. Finned Tube Heat Exchanger (FTHEX).....	12
1.2.2. Plate Heat Exchanger .....	12
1.3. The Objective of the Thesis .....	13
1.4. Thesis Outline.....	14
CHAPTER 2. LITARATURE SURVEY.....	15
2.1. Literature Review.....	15
2.2. Combustion.....	20
2.2.1. Combustion Types .....	21
2.2.1.1. Combustion with Insufficient Air.....	21
2.2.1.2. Combustion with Excess Air.....	21
2.2.1.3. Full Combustion.....	22
2.2.1. Flame Types .....	22
2.2.1.1. Premixed Flames.....	22
2.2.1.2. Diffusion (Non-Premixed Flames).....	23
2.2.1.3. Partially Premixed Flames.....	24
2.3. Combustion Equations.....	25

2.4. Condensation.....	29
CHAPTER 3. TEST RESULTS & CALCULATIONS.....	31
3.1. Mapping Tests Method.....	31
3.2. Test Results and Calculations.....	34
3.2.1. Mapping Results at Min Load & Calculations.....	34
3.2.2. Mapping Results at Max Load & Calculations.....	50
3.3. Validations.....	67
CHAPTER 4. CONCLUSION.....	71
REFERENCES .....	73

## LIST OF FIGURES

<b><u>Figure</u></b>	<b><u>Page</u></b>
Figure 1.1. A Catalytic Heater.....	3
Figure 1.2. Type B – Open Flue (OF) Systems.....	4
Figure 1.3. Assembly drawing of Open Flue (OF) appliance.....	4
Figure 1.4. Type C – Room Sealed Flue (RSF) Systems.....	5
Figure 1.5. Room Sealed Flue (RSF) appliance.....	5
Figure 1.6. Schematic function view of an RSF type Conventional appliance.....	6
Figure 1.7. Schematic function view of a Condensing appliance.....	6
Figure 1.8. Gas Valve .....	7
Figure 1.9. Burner .....	7
Figure 1.10. Ignition Electrode.....	8
Figure 1.11. Ionization Electrode .....	8
Figure 1.12. Combustion Chamber .....	8
Figure 1.13. Primary Heat Exchanger .....	9
Figure 1.14. Fan .....	9
Figure 1.15. Fan Hood .....	10
Figure 1.16. Expansion Vessel.....	10
Figure 1.17. Circulation Pump.....	10
Figure 1.18. Secondary Heat Exchanger.....	11
Figure 1.19. Exploded view of a FTHEX in a combi boiler systems.....	12
Figure 1.20. An example of a Plate HEx working principle.....	13
Figure 2.1. Schematic representation of the simplest way of the combustion process.....	20
Figure 2.2. Premixed Flame .....	22
Figure 2.3. Schematic view of Premixed Flame .....	22
Figure 2.4. Bunsen Burner Methane-Air Premixed Flame.....	23
Figure 2.5. Diffusion Flame.....	23
Figure 2.6. Schematic view of Diffusion Flame .....	23
Figure 2.7. Examples of Diffusion Type Jet Fuels.....	24
Figure 2.8. Partial Premixed Flame.....	24
Figure 2.9. Schematic view of Partial Premixed Flame.....	24

Figure 2.10. Composition of Air.....	25
Figure 2.11. Minor Components in Dry Air.....	25
Figure 2.12. Basic Combustion Reactions.....	26
Figure 2.13. CO <sub>2</sub> in vol. % - Dew Point Water Vapor Graph for Natural Gas.....	29
Figure 3.1. Unscrewed front panel of the B type conventional appliance.....	32
Figure 3.2. Points of the drilling in a hole on the surface for B type appliance.....	32
Figure 3.3. Mapping points on the Cu HEx for B type appliance.....	32
Figure 3.4. Unscrewed front panel of the C type conventional appliance.....	32
Figure 3.5. Mapping points on the Cu HEx for C type appliance.....	32
Figure 3.6. Mapping points on the SS HEx for C type appliance.....	32
Figure 3.7. %CO <sub>2</sub> rate distribution over the Cu HEx at min load (47/53°C) for B type appliance.....	35
Figure 3.8. Temperature distribution over the Cu HEx at min load (47/53°C) for B type appliance.....	38
Figure 3.9. %CO <sub>2</sub> rate distribution over the Cu HEx at min load (47/53°C) for C type appliance.....	46
Figure 3.10. Temperature distribution over the Cu HEx at min load (47/53°C) for C type appliance.....	47
Figure 3.11: %CO <sub>2</sub> rate distribution over the Cu HEx at max load (60/80°C) for B type appliance.....	51
Figure 3.12. Temperature distribution over the Cu HEx at max load (60/80°C) for B type appliance.....	52
Figure 3.13. %CO <sub>2</sub> rate distribution over the Cu HEx at max load (60/80°C) for C type appliance.....	57
Figure 3.14. Temperature distribution over the Cu HEx at max load (60/80°C) for C type appliance.....	58
Figure 3.15. %CO <sub>2</sub> rate distribution over the SS HEx at max load (60/80°C) for C type appliance.....	62
Figure 3.16. Temperature distribution over the SS HEx at max load (60/80°C) for C type appliance.....	63
Figure 3.17. The observation of regional condensation while working the appliance under condensation conditions (C type – 60/80°C at max load).....	67
Figure 3.18. The appearance of regional condensation on the heat exchanger (C type – 60/80°C at max load).....	68

Figure 3.19. A formation of soot after running a long time in condensation conditions.....	68
Figure 3.20. A formation of corrosion after running a long time in condensation conditions.....	69
Figure 3.21. The heat exchanger after the condensation tests .....	70

## LIST OF TABLES

<b><u>Table</u></b>	<b><u>Page</u></b>
Table 2.1. Components of the Natural Gas.....	27
Table 2.2. Composition of Test Reference Gases.....	28
Table 2.3. Dew Point Water Vapor Values Corresponding to CO <sub>2</sub> in vol %.....	30
Table 3.1. Specifications of Material Parameters.....	34
Table 3.2. %CO <sub>2</sub> rate distribution over the B type Cu HEx at min load (47/53°C).....	35
Table 3.3. Temperature distribution over the B type Cu HEx at min load (47/53°C).....	37
Table 3.4. Thermophysical properties of CO <sub>2</sub> , N <sub>2</sub> and O <sub>2</sub> at 147°C.....	39
Table 3.5. Thermophysical properties of Flue gas for the B type Cu HEx at min load (47/53°C).....	39
Table 3.6. Calculation parameters for Re and Nu numbers of Flue Gas side for the B type Cu HEx at min load (47/53°C).....	40
Table 3.7. Heat Exchanger Design Parameters for Cu HEx.....	41
Table 3.8. Calculation parameters Re and Nu numbers of Water Side for Cu HEx.....	41
Table 3.9. Thermophysical properties of water at 50°C.....	42
Table 3.10. Heat Transfer Resistance Calculation Parameters for the B type Cu HEx at min load (47/53°C).....	43
Table 3.11. Gas Temperature Results for the B type Cu HEx at min load (47/53°C).....	43
Table 3.12. Mean Water Temperature Change Calculations for the B type Cu HEx at min load (47/53°C).....	44
Table 3.13. Regional Water Temperatures at Risky Area for the B type Cu HEx at min load (47/53°C).....	44
Table 3.14. Regional Pipe Outer Surface Temperatures at Risky Area for the B type Cu HEx at min load (47/53°C) for Cu HEx.....	45
Table 3.15. %CO <sub>2</sub> rate distribution over the C type Cu HEx at min load (47/53°C).....	45

Table 3.16. Temperature distribution over the C type Cu HEx at min load (47/53°C).....	47
Table 3.17. Thermophysical properties of Flue gas for the C type Cu HEx at min load (47/53°C).....	48
Table 3.18. Results for Re and Nu numbers and h value of both Flue Gas and Water Side for the C type Cu HEx at min load (47/53°C).....	48
Table 3.19. Heat Transfer Resistance and Gas Temperatures Results for the C type Cu HEx at min load (47/53°C) .....	49
Table 3.20. Regional Water and Pipe Outer Surface Temperatures at Risky Area for the C type Cu HEx at min load (47/53°C).....	49
Table 3.21. %CO <sub>2</sub> rate distribution over the B type Cu HEx at max load (60/80°C).....	50
Table 3.22. Temperature distribution over the B type Cu HEx at max load (60/80°C).....	52
Table 3.23. Thermophysical properties of CO <sub>2</sub> , N <sub>2</sub> and O <sub>2</sub> at 357°C.....	53
Table 3.24. Thermophysical properties of Flue gas for the B type Cu HEx at max load (60/80°C).....	53
Table 3.25. Thermophysical properties of water at 70°C.....	54
Table 3.26. Results for Re and Nu numbers and h value of both Flue Gas and Water Side for the B type Cu HEx at max load (60/80°C).....	54
Table 3.27. Heat Transfer Resistance and Gas Temperatures Results for the B type Cu HEx at max load (60/80°C).....	55
Table 3.28. Regional Water and Pipe Outer Surface Temperatures at Risky Area for the B type Cu HEx at max load (60/80°C).....	55
Table 3.29. %CO <sub>2</sub> rate distribution over the C type Cu Hex at max load (60/80°C).....	56
Table 3.30. Temperature distribution over the C type Cu HEx at max load (60/80°C).....	58
Table 3.31. Thermophysical properties of CO <sub>2</sub> , N <sub>2</sub> and O <sub>2</sub> at 325°C.....	59
Table 3.32. Thermophysical properties of Flue gas for the C type Cu HEx at max load (60/80°C).....	59
Table 3.33. Results for Re and Nu numbers and h value of both Flue Gas and Water Side for the C type Cu HEx at max load (60/80°C).....	60



Table 3.34. Heat Transfer Resistance and Gas Temperatures Results for the C type Cu HEx at max load (60/80°C).....	60
Table 3.35. Regional Water and Pipe Outer Surface Temperatures at Risky Area for the C type Cu HEx at max load (60/80°C).....	61
Table 3.36. %CO <sub>2</sub> rate distribution over the C type SS HEx at max load (60/80°C).....	61
Table 3.37. Temperature distribution over the C type SS HEx at max load (60/80°C).....	63
Table 3.38. Thermophysical properties of Flue gas for the C type SS HEx at max load (60/80°C).....	64
Table 3.39. Calculation parameters and results for Re and Nu numbers and h value of Flue Gas side for the C type SS HEx at max load (60/80°C).....	64
Table 3.40. Heat Exchanger Design Parameters for SS HEx.....	65
Table 3.41. Results for Re and Nu numbers and h value of Water Side for the C type SS HEx at max load (60/80°C).....	65
Table 3.42. Heat Transfer Resistance Calculation Parameters for the C type SS HEx at max load (60/80°C).....	65
Table 3.43. Gas Temperature Results for the C type SS HEx at max load (60/80°C).....	66
Table 3.44. Regional Water and Pipe Outer Surface Temperatures at Risky Area for the C type SS HEx at max load (60/80°C).....	66
Table 4.1. Comparison results between B type and C type appliances.....	71
Table 4.2. Comparison results between heat exchangers with Cu fin and SS fin.....	72

# LIST OF SYMBOL

## Abbreviations

PHE <sub>x</sub>	Primary Heat Exchanger
SHE <sub>x</sub>	Secondary Heat Exchanger
OF	Open Flue
RSF	Room Sealed Flue
HE <sub>x</sub>	Heat Exchanger
FTHE <sub>x</sub>	Finned Tube Heat Exchanger
max	maximum
min	minimum

## Symbols

SS	Stainless Steel
Cu	Copper
CO <sub>2</sub>	Carbon Dioxide
CO	Carbon Monoxide
N <sub>2</sub>	Nitrogen
O <sub>2</sub>	Oxygen
CH <sub>4</sub>	Methane
Q <sub>i</sub>	Heat input
H <sub>i</sub>	Net calorific value
Q <sub>o</sub>	Heat output
$\dot{V}$	Volumetric flow rate
T	Temperature
Pr	Prandtl number
k	Thermal conductivity
A	Area
v	Velocity
Re	Reynolds number
Nu	Nusselt number
h	Heat transfer coefficient
S	Surface

D	Diameter
$D_h$	Hydraulic diameter
$H$	Fin height
Y	Fin pitch
$R_f''$	Representative Fouling Factor
R	Thermal resistance
U	Overall heat transfer coefficient
$\dot{m}$	Mass flow rate
$C_p$	Specific heat capacity

### Greek Letters

$\phi$	Stoichiometric region
$\lambda$	Excess air ratio
$\eta$	Efficiency
$\rho$	Density
$\mu$	Dynamic viscosity
$\delta$	thickness

### Subscripts

fg	Flue gas
f	Fin
p	Pipe
w	Water
pi	Pipe inner
po	Pipe outer
o	Overall
cg	Combustion gas
pos	Pipe outer surface

# CHAPTER 1

## INTRODUCTION

This section describes the combi boilers, the area of usage of them, and the components that make the combi boilers, the definition of the heat exchanger and areas of usage of it. In addition, the emergence of the subject of the thesis and the outlines of the thesis are also included.

### 1.1. Combi Boiler

Combi word is the abbreviation of the combination word. Combi boilers are heating appliances which are used in enclosed areas such as residential and office to meet the heating needs and provide domestic hot water comfort. Because of their small size and wall hanging, they occupy less space and are suitable for small-scale areas such as residential and office. Nowadays, the popularity of this type of appliance, while meeting user demand for heating, increased due to both silent operational conditions and offering only the possibility of paying according to usage compared to other types of heating. The appliance performs this heating operation in the combustion chamber by combines the natural gas with the oxygen which is taken from the air. The usage of natural gas as a fuel has also increased the use of these appliances. Because it is different from boiler systems, considering all these properties, the definition is actually Gas-Wall Hang Heating Appliances.

The basic function of the combi boiler is to meet the required space heating requirement. In case of user's request, the appliance provides to adjust the comfort of domestic hot water. While the unit performs its first function, the central heating water is sent to the radiators by heating in the primary heat exchanger (PHEx), with the aid of the pump and the required space heating is provided. This process works as a closed-loop system. The appliance performs this heating operation in the combustion chamber by combine the natural gas with the oxygen which is taken from the air.

When the function of the combi boiler is to adjust the comfort of domestic hot water, the water which is heated in the PHEx reaches the user by transferring its heat to

the usage water in the plate heat exchanger which is named as the secondary heat exchanger (SHEx) in this study.

### **1.1.1. Categorized of the Combi Boilers**

Combi boilers are categorized into several types according to its very different properties.<sup>1</sup>

- According to drawing fresh air and discharge of exhaust gases
  - Type A
  - Type B – Open Flue (OF) Appliances
  - Type C – Room Sealed Flue (RSF) Appliances
- According to flue gas recovery
  - Conventional (Type B or C)
  - Condensing (Type C only)
- According to operating environment
  - Indoor
  - Outdoor
- According to ignition system
  - Pilot Flame
  - Electronic Ignition
- According to heat exchanger type
  - Monothermal Boilers – Hot water exchanger which is separated from main heat exchanger
  - Bi-thermal Boilers – Heated hot water in the primary heat exchanger
- According to fuel type
  - Natural Gas
  - LPG
- According to capacity
  - Capacity of 17.000 - 20.000 kcal/h
  - Capacity of 24.000 - 25.000 kcal/h
  - Capacity of 27.000 - 30.000 kcal/h

- According to NOx emission ratio
  - Low NOx Emission
  - Medium NOx Emission

Common usages to categorize of this appliances are according to drawing fresh air and discharge of exhaust gases and according to flue gas recovery.

According to drawing fresh air and the discharge of exhaust gases, combi boilers are categorized into three different types, A, B and C types.

#### 1.1.1.1. Type A

Such appliances, combine the fuel gas with the oxygen which is taken from the place where the appliance installed and then leave the combustion gases in the environment they are still in. Although they are not included in today's combi boilers, in the literature they are still counted in the combi boiler types. As an example, we can give the catalytic heater.



Figure 1.1. A Catalytic Heater<sup>2</sup>

#### 1.1.1.2. Type B – Open Flue (OF) Appliance

The OF type combi boilers combine the combustion gas with the oxygen required for combustion, which is taken from the room they are installed, to perform the combustion process in the combustion chamber. The exhaust gas formed through combustion is discharged from the building chimney. This type of combi boilers name as Type B which is shown in Fig. 1.2. Combi boilers with this type of flue are ***Conventional*** type combi boilers. There is no use of type B chimneys in condensing type combi boilers.

The duct which the exhaust gas is passed to the chimney must be leak-proof and steel. Normally exhaust gas is evacuated by rising via heat consisted the result of the combustion process. The room must be well ventilated since the air required to perform

the combustion process is taken from there. Installation of this type appliances in bathrooms and small-space areas is not suitable. Chimney maintenance must be done to prevent carbon monoxide poisoning.

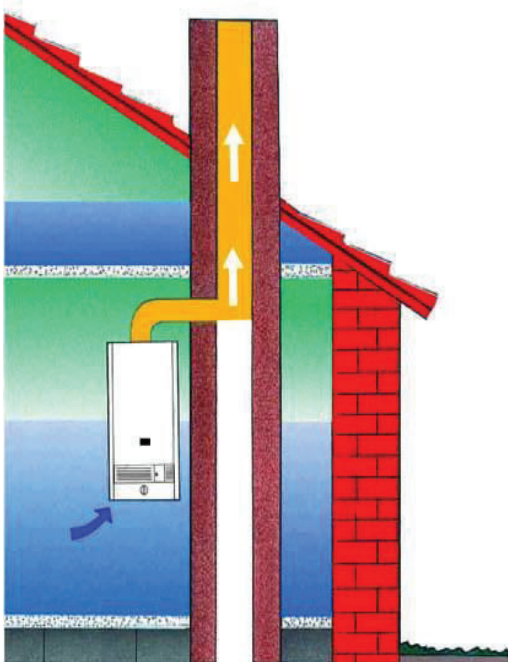


Figure 1.2. Type B – Open Flue (OF) Systems<sup>3</sup>



Figure 1.3. Assembly drawing of Open Flue (OF) appliance<sup>3</sup>

### 1.1.1.3. Type C – Room Sealed Flue (RSF) Appliance

The RSF type combi boilers draw the air from the outside to be used for the combustion from a part of the chimney set by using a fan and discharge the combustion gases to outside through the other part of the chimney set by using of the same fan. Since all these gas and air exchanges are carried out with outdoor environment, it is absolutely necessary for the appliance to be connected to the outside environment. Since they are independent of the environment they are in, there is no need to ventilate the room where it is installed. Such appliances are ideal for installations that are not suitable for chimney use because they do not need building chimneys.

The appliances of the RSF type are divided into two as *conventional* and *condensing* combi boilers. Although the basic operating principles of conventional and condensing appliances of the RSF type are similar, the combustion chamber, the main exchanger system and the chimney duct material differs because the heat is recovered in the condensing appliances. OF or RSF type conventional combi boilers have the similar

combustion chambers and main exchanger types. Unlike conventional appliances, the condensing type combi boilers do not have an open combustion chamber, the combustion chambers of these appliances are in the form of a hermetic closed cell.

For both conventional and condensing combi boilers in RSF type, the flow type is forced circulation and fan is used. The chimney set is made up of two internal pipes which are concentric. The air is taken from the outside of the pipe while the exhaust gas is evacuated from the inside of the pipe. In conventional types, steel material is used for inner flue pipe whereas inner flue pipe of condensing types is plastic material.

The RSF type appliances are also known as *hermetic* type appliances.

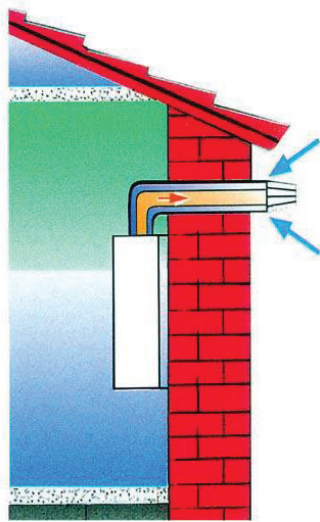


Figure 1.4. Type C – Room Sealed Flue (RSF) Systems<sup>3</sup>

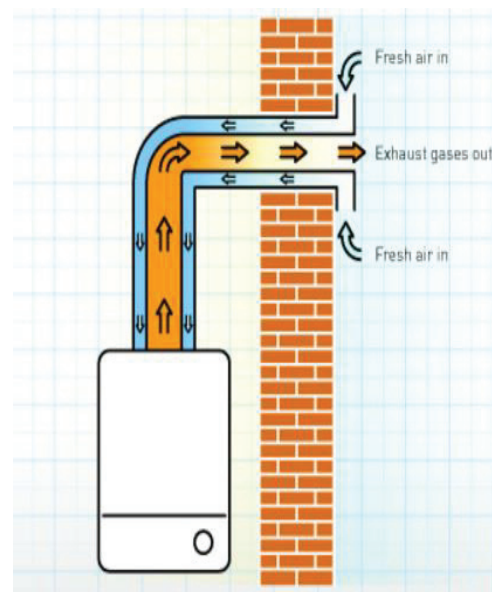


Figure 1.5. Room Sealed Flue (RSF) appliance<sup>4</sup>

In conventional appliances, the water vapor produced after the combustion process is thrown into the atmosphere together with the flue gas. In this case, the hidden energy in the water vapor is not used.

The condensing appliances are intended to use the water vapor in the flue gas. The main heat exchanger, which has a large size and is in the shape of a heat cell, condense the water vapor in the flue gas and to increase the temperature of the inlet water by using the heat generated during the condensation. The resulting condensation water is acidic and is discharged through the condensation vessel inside the appliance as it is harmful to the environment.



Condensing appliances operate on average 15% more efficient than conventional appliances since they use a large part of the flue gas heat in the heating process.

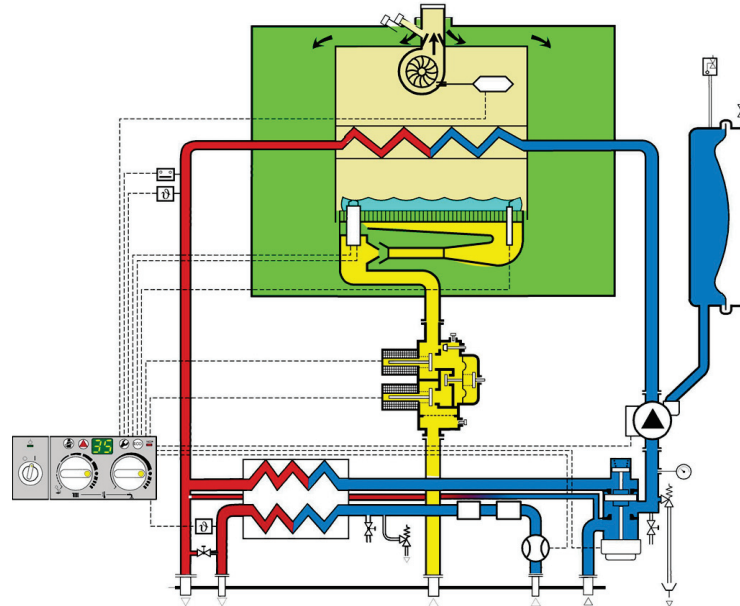


Figure 1.6. Schematic function view of an RSF type Conventional appliance<sup>3</sup>

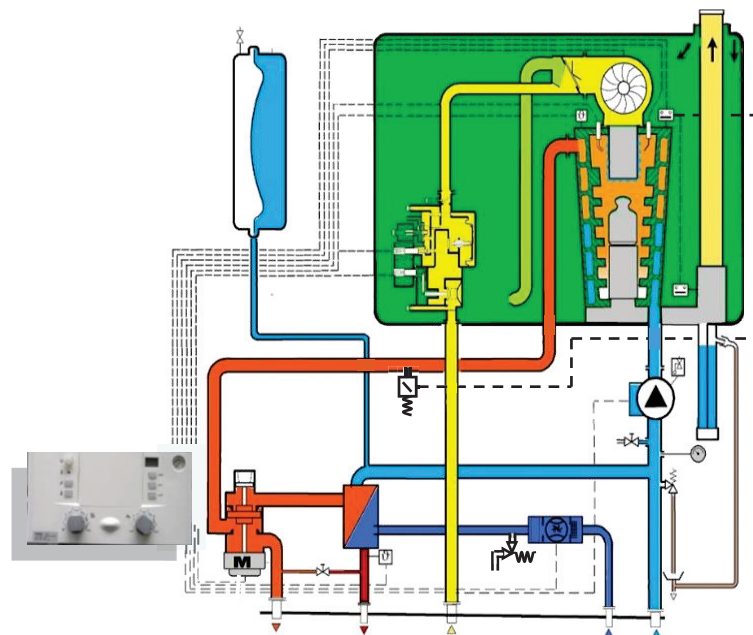


Figure 1.7. Schematic function view of a Condensing appliance<sup>3</sup>

### 1.1.2. The Components of the Conventional Combi Boilers

In this thesis, RSF type conventional combi boilers are studied. This is why the conventional appliance is selected when introducing the components of the combi boiler. Condensing appliances are mentioned briefly above.

#### 1.1.2.1. Gas Valve

The gas valve regulates the amount of fuel gas required for combustion to be introduced into the burner. The modulation of the gas valve and opening/closing of it are controlled by the appliance's main board. It performs this function by moving coils in it. Since the height of the flame length, the efficiency of the appliance and domestic hot water comfort depends on the gas modulation, this function is very important.

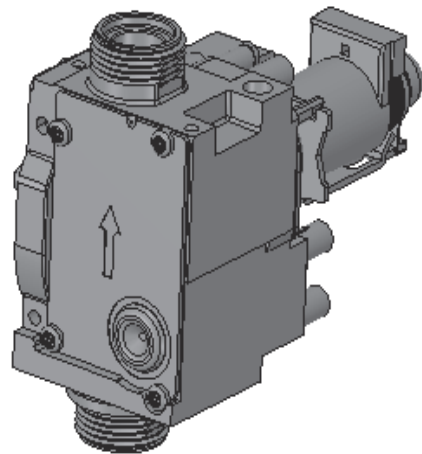


Figure 1.8. Gas Valve<sup>3</sup>

#### 1.1.2.2. Burner

The burner is the place where the combustion fuel coming from the gas valve to the injectors through the manifold and mixes with the air. Thanks to the ignition electrode on the burner, combustion is realized on the burner. It is the part of where is included the manifold and the injectors.

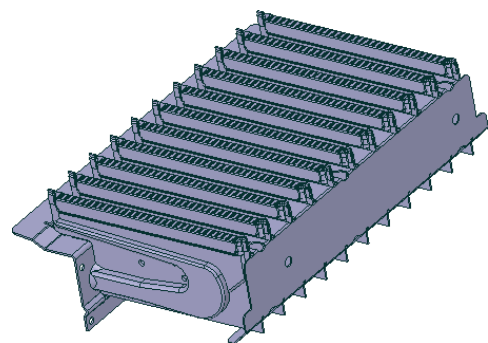


Figure 1.9. Burner<sup>3</sup>

### 1.1.2.3. Ignition Electrode

Ignition electrode is the component which ignites in the burner the combustion gas coming from the gas valve, with the warning from the main board or spark generator. The working principle is based on creating an arc between the electrodes by generating the high voltage. This arc creates a spark and ignites the combustion gas mixture.

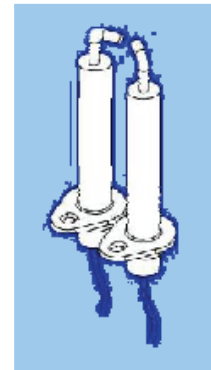


Figure 1.10. Ignition Electrode<sup>3</sup>

### 1.1.2.4. Ionization Electrode

Ionization electrode is used as a combustion sensor and with ignition electrode together in the same system. After seeing the flame formation gives this information to the card and stops the ignition.

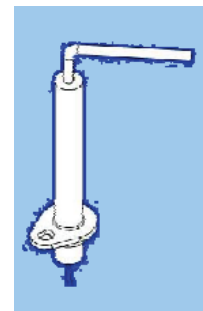


Figure 1.11. Ionization Electrode<sup>3</sup>

### 1.1.2.5. Combustion Chamber

It is the name of the closed and insulated room where gas and air are mixed and burned in the burner. To ensure insulation, the walls of the room are made of fire-resistant refractory bricks.



Figure 1.12. Combustion Chamber<sup>3</sup>

#### 1.1.2.6. Primary Heat Exchanger

In the case of the conventional combi boiler systems; the cold water passing through the piping is heated by heat from the combustion gases coming into contact with the surface of pipes and the fins around the pipes and is used as both space heating and helping to heat domestic hot water. Finned tube heat exchanger is used as the primary heat exchanger.

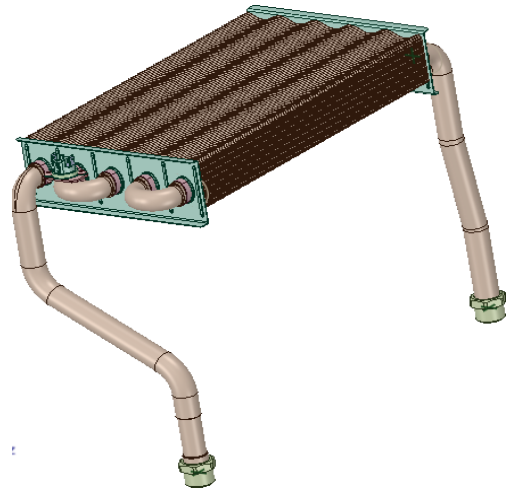


Figure 1.13. Primary Heat Exchanger<sup>3</sup>

#### 1.1.2.7. Fan

In RSF appliances, the fan draws the fresh air from the outside of the room for the combustion process and discharges the exhaust gas which is produced after the combustion through the chimney. The fan is one of the two most important parts of the system together with the gas valve due to the modulation feature.

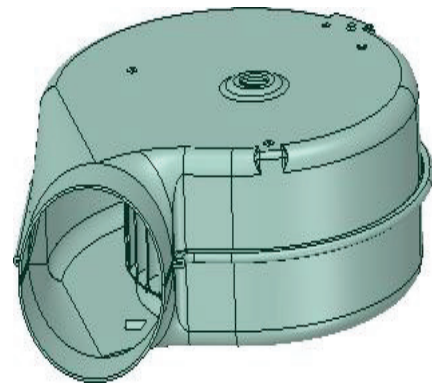


Figure 1.14. Fan<sup>3</sup>

Thanks to the modulating feature, when the fan speed changes, the amount of fresh air entering the combustion chamber also changes and an efficient combustion occurs. When the amount of incoming fresh air is low, the fuel gas is exhausted without being used completely, whereas when it is too high, the consisted heat in the combustion cools due to high amount fresh air.

### 1.1.2.8. Fan Hood

The fan hood, allows the exhaust gases to mix with the air and directs the mixture to the inlet of the fan to blow out from the chimney. In addition, it is also an obstructive feature for the backlash that can occur under adverse wind conditions.

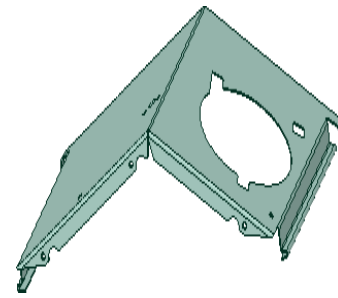


Figure 1.15. Fan Hood<sup>3</sup>

### 1.1.2.9. Expansion Vessel

The expansion vessel acts as a pressure balancing mechanism to prevent damage to mechanical and pipeline components in the system due to the high pressure of the heated water.

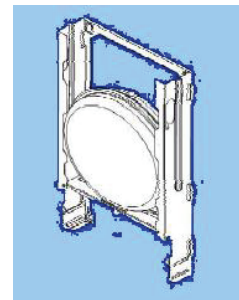


Figure 1.16. Expansion Vessel<sup>3</sup>

### 1.1.2.10. Circulation Pump

The circulation pump supplies water from the system to heat exchangers for warming up, and then allows the circulation of water between boilers and radiators. It is important to choose the proper pump according to the pump head and the flow rate. Installation care is important for this component as it may result in congestion resulting from calcification or deposition.

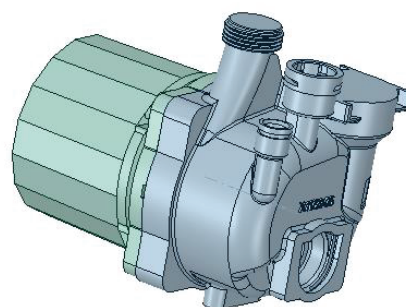


Figure 1.17. Circulation Pump<sup>3</sup>

### 1.1.2.11. Secondary Heat Exchanger

The secondary heat exchangers are used for heating the domestic hot water in the combi boiler systems. Plate heat exchanger is used as the secondary heat exchanger.

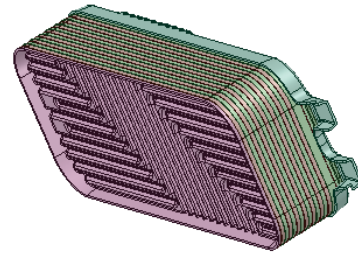


Figure 1.18. Secondary Heat Exchanger<sup>3</sup>

## 1.2. Heat Exchangers (HEX)

The heat exchange process happens between fluids at different temperatures separated by a solid wall.<sup>5</sup> Heat exchangers (HEX) is an appliance where this heat exchange takes place. Analysis and design of the heat exchangers consist both conduction and convection and neglect the radiation. It is because for radiative transfer between the exchanger and environment, the heat exchangers are usually uninsulated and their external surfaces are not very hot.<sup>6</sup>

Heat exchangers can be used for different aims in a variety of applications, such as steam generators in thermal power plants, evaporators, and condensers in heating, ventilating and air conditioning (HVAC) applications, distillers in chemical industry and refrigeration process, electronic heat sinks, automobile radiators, and regenerators in gas turbine engines.<sup>7</sup>

In the combi boiler systems, there are two types of heat exchanger usage which are about the primary heat exchanger and secondary heat exchanger.

Primary heat exchangers are finned tube heat exchangers in conventional appliances, while heat cells in condensing appliances.

Plate heat exchangers are used as secondary heat exchangers in combi boilers.

### 1.2.1. Finned Tube Heat Exchanger (FTHEx)

The finned tube heat exchangers comprise tubes with fins placed in the outer surface areas. Creating additional space around the pipe by using fins allows increasing the rate of heat transfer.<sup>8</sup>

Finned tube heat exchangers are widely used in car radiators, industrial heat exchangers, and various home appliances. In use such as car radiators and air conditioning systems, it is intended that the hot water in the pipes be cooled by being exposed to the flow of cold air.<sup>9</sup>

In the case of the conventional combi boiler systems; the cold water passing through the piping is heated by heat from the combustion gases coming into contact with the surface of pipes and the fins around the pipes and is used as both space heating and helping to heat domestic hot water.

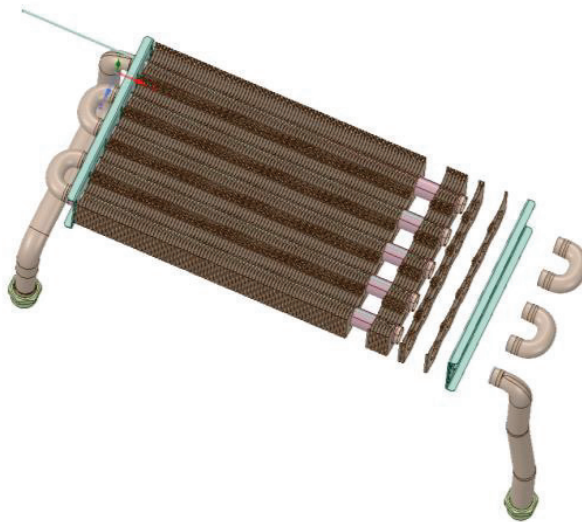


Figure 1.19. Exploded view of a FTHEx in a combi boiler systems<sup>3</sup>

### 1.2.2. Plate Heat Exchanger

The plate heat exchangers consist of a series of parallel plates which are stacked on top of one another so that there is enough space between the two adjacent plates to allow the flow channels to flow between them.<sup>10</sup>



Plate heat exchangers are small in volume and have a very high heat transfer area compared to their volume. It takes up very little space, especially compared to fin and tube type heat exchangers.<sup>11</sup>

The plate heat exchangers are used for heating the domestic hot water in the combi boiler systems. According to other types of heat exchangers, it is necessary to use a strainer because the problem of clogging is more visible.

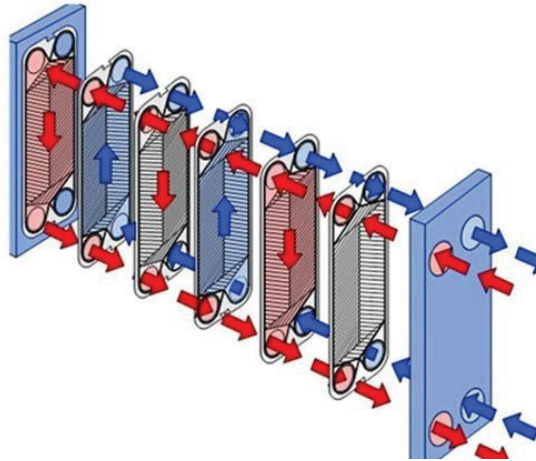


Figure 1.20. An example of a Plate HEX working principle<sup>12</sup>

### 1.3. The Objective of the Thesis

In conventional combi boilers, the condensation occurrence is undesirable, and over time it causes corrosion in the main heat exchangers, which decrease the efficiency and the lifetime. For these types of appliances, life tests are performed to check if corrosion has occurred or not over time. But life tests take a long time and require the high cost. The purpose of this thesis is to find a general heat transfer correlation and to use the calculation method instead of the long-running life tests.

Firstly the conditions under which the condensation has occurred on the main exchanger of conventional type combi boiler will be identified by making tests. The study will be carried out to investigate two different topics on three different appliances with different design parameters. As the first topic, influences of the fresh air amount on both combustion and condensation will be determined in conventional appliances of Type B and Type C. The other topic is to find the effects of the exchanger design parameter changes on condensation using two different fin materials as the copper (Cu) fin and



stainless steel (SS) fin, and using different exchanger sizes. Mapping tests will be performed for these studies and the carbon dioxide (CO<sub>2</sub>) percentages and temperature distributions from mapping tests will be used in the calculation. Critical temperature values will be found for condensation after calculations and these values are used in condensation preventive works.

## **1.4. Thesis Outline**

In the first chapter of this work, which consists of four main chapters, combi boiler appliances and types are explained and the main components of the combi boilers are introduced. Also, the heat exchangers which are discussed during this study as the main topic are mentioned in general terms and are introduced the two types of heat exchangers which are used in combi boilers. In addition, it is explained the objective of the study and progress of this thesis as content.

In the next part, it is mentioned about the similar studies in literature in general and the combustion theories in combi boilers and condensation.

In chapter three, the mapping test method was explained. Mapping results of flue gas CO<sub>2</sub> percentages and temperature distributions obtained under different test conditions were shared. Heat transfer calculations made using these results were explained. And validation results were explained with visuals.

In the last chapter, chapter four, the net outputs of the thesis study are presented.

## CHAPTER 2

### LITARATURE SURVEY

In the literature, there are generally numerical studies on heat exchangers. It is because of that the experimental studies have the high cost, required a long time and not applied in some complex problems. But experimental work is more effective because of its reliable results that reflect the reality.

In the following part, it is mentioned about the similar studies in literature in general and the combustion theories in combi boilers and condensation.

#### 2.1. Literature Review

Wang et al.<sup>13</sup>, researched performance effect by performing heat transfer and pressure drop tests on a wavy fin and tube heat exchanger. During the study, they used 18 different wavy fin and tube exchangers with different fin ranges, tube rows, and flow arrangements. Experiments were made in the wind tunnel and during the experiments, the Reynolds number values were taken from between 400 and 8000. At the end of the study, the effect of the fin range variable on the Colburn factor and the effect on the friction factor of the tube rows variable were found to be negligible. It has been found that wavy fin geometry increase the heat transfer between 55-70% and friction factor between 66-140% compared to plain fin.

Jang et al.<sup>14</sup>, studied the effects of the tube arrangement, the number of tube rows and variable fin pitch on fluid flow and heat transfer, depending on the variable Reynolds numbers in the plate-fin and tube heat exchanger. In this study, the Reynolds number is between 60 and 900, the fin pitch is between 8 and 12 per inch, and the tube row is between 1 and 6. The average Nusselt number has decreased as the number of rows of tubes increased from 1 to 6, and the effect on the heat transfer coefficient has become negligible when the number of rows of tubes increased above 4. As regards tube arrangements in this study, staggered arrangements increase heat transfer by 15-27% compared to in-line regulation, while at the same time it increases pressure drop by 20-25%.

Bilir et al.<sup>15</sup>, studied the effect of some fin parameters on combi boiler heat exchanger on heat transfer and pressure drop by taking reference one of the commercial combi boiler heat exchanger. The fin parameters discussed are fin, fin tube, and protrusion of the fin. This work is done as a numerical and the name of the CFD program used in the study is "Ansys Fluent". One of the combinations created from these parameters is presented as the best option.

Chang and Wang<sup>16</sup> aimed to find a heat transfer correlation by examining different geometrical parameters such as louver angle, tube width, louver length, louver pitch, fin length and fin pitch. They investigated 91 samples of louvered fin heat exchangers in their study. They found that about 90% of the geometries studied for corrugated louver fin geometry exhibit a  $\pm 15\%$  similarity with an average deviation of 7.5%. If plate-and-tube louver fin data is used in that correlation, the deviation increases to 8.2%.

Li and Norris<sup>17</sup> conducted analytical and experimental studies on flue gas formed in condensing heat exchangers. The aim of this study is to establish an analytical model for estimating the condensation rate of the water vapor in the flue gas and amount of the heat transfer from the flue gas to the cooling water by using some parameters such as the flue gas outlet temperature, the cooling water outlet temperature, the water vapor mole fraction and condensation rate of the water vapor. They aimed at forming a heat and mass transfer model for this process.

Bilirgen et al.<sup>18</sup>, studied numerically effects of the fin spacing, the fin height, the fin thickness and the fin material on the overall heat transfer and pressure drop, for a single row of finned tubes in crossflow. As a result of the study, they found a direct relationship between overall heat transfer and fin spacing. A similar relationship exists between fin height and pressure drop. Though fin thickness and material thermal conductivity have an increasing effect on pressure drop and heat transfer, this effect is small.

Seo et al.<sup>19</sup> investigated experimentally and numerically the characterization of catalytic heat exchangers, heat generation, and heat exchange equipment. According to the experimental results, the most important effect of the catalytic combustion performance is the inlet velocity of the mixture. Other factors are the inlet temperature and equivalence ratio. They stated that the catalytic fin thickness and numbers should be designed to be less than 1 mm and above 6 pieces/inch to obtain the best yield in catalytic heat exchangers.

Kaya et al.<sup>20</sup> aim to solve the boiling problem with the optimization of welding size in finned-tube special heat exchangers in this study. As a result of the CFD analysis, it is found that the welded fittings cooled the water instead of heating it. Another aim of study is to prevent the boiling by increasing the size of the welded fittings. It is found that even when the max welding width was used, boiling of water could not be prevented.

Wang et al.<sup>21</sup> conducted experimental studies on the airside performance of compact slit fin-and-tube heat exchangers. According to the test results, it was found that the number of tube rows and fin pitches did not significantly affect this performance. They concentrated their work on slit-fin geometry and performed tests on the louver surface and the plain fin with comparison methods. They found that intermittent fin surfaces such as louver and slit give higher performance than plain fin surfaces. After the result of studying with 56 different samples, a converging correlation was found. In this correlation, the deviation for heat transfer is 7.26% while the deviation for friction is 7.18%.

Kuvannarat et al.<sup>22</sup> experimentally studied the effect of fin thickness on the airside performance of wavy fin-and-tube heat exchangers under dehumidification conditions. In experiments performed with 10 different samples, they examined the heat transfer performance of the air side using humid air. Because of the interaction between the air and the droplets of condensing water, they have seen vortices in the air flow. It was stated that the heat transfer performance was increased because these vortices form in the main flow in the channel at low wavy intervals. At the end of the study, the proposed correlation for airside performance in wavy fin structure has deviation 7.9% for heat transfer correlation and 7.7% for friction correlation.

Pirompugd et al.<sup>23</sup> had been working on reducing the experimental process in fin and tube heat exchangers under dehumidification conditions. Throughout the study, they had investigated the heat and mass transfer characteristics of such heat exchangers and had focused on some data reduction methods. The data reduction methods examined were the original Threlkeld method, the direct method, the equivalent dry-bulb method, the tube by tube method, the fully wet and fully dry tiny circular fin method, and the finite circular fin method.

Eldeeb et al.<sup>24</sup> examined the available heat transfer and pressure drop correlations for flow boiling and condensation in plate heat exchangers. They applied different refrigerants to those correlations and presented comparative tables. They used refrigerants for 6 different condensation and boiling heat transfer correlations. Ammonia, which

provides the most efficient heat transfer performance among the refrigerants they use (Ammonia, R1234yf, R134a, R32, and R410A). It was thought that the results will shed light on future studies although showing contradictions with the experimental results in the literature. The studies were made numerically and recommended to be supported experimentally.

Dal<sup>25</sup> made numerical studies on the effects of heat transfer and pressure drop by changing parameters of fin and pipe structure in plain fin and tube heat exchanger in his thesis study. In the model variations, the effect of the fins angle on the vertical axis, the distance between the fins and the axial distance variation of the pipes was investigated. As the slope angle increases, the distance between the fins decreases, which increases the speed of the flue gas passing through that area and the heat transfer increases. At the same time, even if the pressure drop increases, the energy required to compensate is less than the heat transfer obtained. He stated that the results of the study are in parallel with the literature and could be used for future studies.

Yang et al.<sup>26</sup> studied single-phase heat transfer on a brazed-plate type heat exchanger in experimental. In the experiments, 9 heat exchangers with different geometries and high Prandtl number fluids were used. As a result of the experiments, correlations were obtained for each different heat exchanger model and general one. They found that the largest factor influencing these correlations was the herringbone angle and heat transfer was highly influenced by geometric dimensions. Correlations were found to be different from the literature. The general correlation found is 50% accuracy and it is mentioned that the experiment numbers should be increased to reach more convergent correlations.

Wang and Chi<sup>27</sup> examined the effects of the number of tube rows, the fin pitch and the tube diameter on the thermal-hydraulic characteristics for airside performance in fin-and-tube heat exchangers with plain fin configurations. After the 18 samples examined, according to the number of tube rows, the heat transfer performance increased while the fin pitch was decreased. In these examination conditions, they also observed that the effect of tube rows on friction was very small. The fin pitch was found as the most important variable and the pressure drop was observed approximately 10-15%.

In this study, Wang et al.<sup>28</sup> found a correlation for the exchanger structure they used in their previous study which is described above paragraph. In this study conducted on 74 samples, the heat transfer correlation confirms 88% of the literature with a deviation

of approximately 7.5%, while the friction correlation confirms 85% of the literature with a deviation of approximately 8.3%.

Karthik et al.<sup>29</sup> conducted a statistical based study on parameter changes that could catch different frontal air velocities on the heat exchanger. They used fin pitch, transverse tube pitch, longitudinal tube pitch, louvered pitch and louver angle as variable parameters in their CFD analysis program. They observed that the experimental results were in good agreement with the analysis results. They concentrated on pressure drop and heat transfer coefficient in their analysis. They noted that the results of the analysis would reduce the time and the cost of the experiments spent for heat exchanger optimization.

Vignali<sup>30</sup> made a life cycle comparison by examining traditional and condensed boiler technologies in his work. He carried out his research on two different brands in Italy with different climate and energy classes. In the analysis results, he found that the condensing boiler appliance affected the environment 23% less than the conventional boiler appliance. As the reason for this, he shows that the condensing boiler appliance release the environment in low-level of carbon monoxide and NO<sub>x</sub>, in addition, has lower fuel consumption.

Liu et al.<sup>31</sup> performed numerical analyzes of large fin pitches on perforated fins in finned and tube heat exchangers on increasing air-side heat transfer performance. They examined perforation size and number, heat transfer rates of the FTHE<sub>x</sub>, and different large fin pitches. According to numerical simulations of perforated FTHE<sub>x</sub>s with an optimal perforation design, where perforations can be seen with a maximum increase compared to a non-perforated FTHE<sub>x</sub> plate, are seen in the results. As a quick note to note, the total heat transfer surfaces decrease with perforations in perforated FTHE<sub>x</sub>, which leads to a reduction in heat transfer rates. Two methods have been proposed to compensate the total surface for perforated FTHE<sub>x</sub>.

Čarija et al.<sup>32</sup> made the air flow and the heat exchange analyze for the air side in a multi-row flap heat exchanger. They made a comparison depending on the flat and louvered blades and the fin and heat exchanger characteristics on Reynolds number in finned and tube heat exchanger. The results of the louvered heat exchanger calculations give better data for heat transfer characteristics. According to results pressure drop is higher than the flat fin heat exchanger. The computational fluid dynamics (CFD) results were validated with experimental results. There is an acceptable Nusselt number deviation and pretty much the same Pressure drop value.

## 2.2. Combustion

The combustion reaction is a chemical reaction that occurs as a result of fuel and oxidant entering the reaction. The fuel is usually hydrocarbon, while the oxidant is air. The oxidized products resulting from the combustion reaction are carbon monoxide (CO) and water, while the energy released after this process is heat and light.<sup>33</sup>

Energy is required in the first stage as it is in the case of wood fire to begin the combustion reaction. The wood in the environment of oxygen is not subject to spontaneous combustion, but the activation energy must be exceeded in order to start the reaction. Often, a flame process is used to exceed the necessary activation energy threshold. Due to the heat released during this reaction, the reaction can proceed on its own.<sup>34</sup>

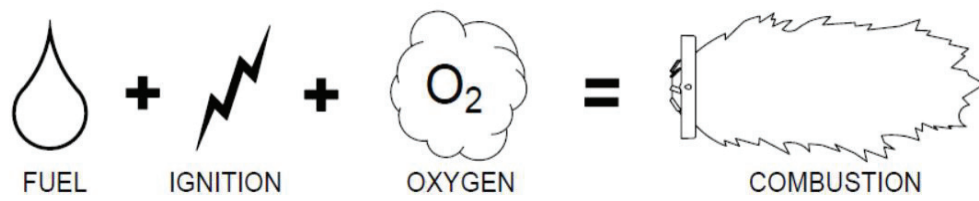


Figure 2.1. Schematic representation of the simplest way of the combustion process<sup>35</sup>

If the heat generated by the reaction is high enough to allow to reveal the perceptible light of the elements entering the reaction, a fire will emerge.

Basically, combustion is the process by which a fuel reacts with a reactive element, such as oxygen, to form an oxidation to release energy, which is released as heat. Burning releases the heat because it is an exothermic reaction. The reason for the release of this heat is that the bonds between the resulting carbon dioxide and water molecules are stronger than the bonds between the oxygen atoms entering the reaction. The formation of these strong bonds leads to energy release.<sup>36</sup>

Sometimes this reaction proceeds very slowly, as in the case of iron corrosion, so temperature change and burning may not be noticeable. Iron also rusts with oxidation, but this process is very slow compared to carbon. We can only see the rust after a long period of time.<sup>37</sup>

The combustion reaction is regarded as one of the first reactions that humanity has under control it.

### **2.3.1 Combustion Types**

The most important factor determining combustion characteristics is that the amount of air required for combustion to occur is low, very high or as necessary.

For this reason, combustion is named according to the air in the fuel-air mixture:

- 1) Combustion with insufficient air,
- 2) Combustion with excess air,
- 3) Full combustion

#### **2.3.1.1. Combustion with Insufficient Air**

The combustion with insufficient air means that the air does not enter the reaction enough to make the fuel burn in accordance with the theoretical combustion equation. It has a darker flame color compared to the normal.<sup>38</sup>

Oxygen is completely unable to bond to carbon monoxide because of the small amount of air entering the reaction and this causes to release excess carbon monoxide from the flue. This will reduce heat transfer by causing soot and fouling to accumulate on the heat transfer surfaces. Failure to achieve full combustion will also be reflected in fuel wastage. Because of the carbon monoxide is poisonous gas, this damages both human health and the environment.

#### **2.3.1.2. Combustion with Excess Air**

The combustion with excess air means that the drawn air to make the fuel burn is more than needed, in accordance with the theoretical combustion equation. It has a light and bright flame color compared to the normal.<sup>38</sup>

In the case of excessive air combustion, the flue gas temperatures are high and the combustion chamber temperatures are low. Because when too much air is drawn, excess air that can not enter the reaction will absorb the heat of the burning and cause the efficiency to drop. So we have to burn more fuel to get the same amount of steam.



### 2.3.1.3. Full combustion

Full combustion is the case where there is no combustible gas in the resulting part of the combustion equation. The absence of CO gas in the flue gas is an indication of this.

Generally, the total amount of CO in the flue gas is close to zero and the CO<sub>2</sub> ratio is at the level of 12-13%. Nitrogen gas is also available.<sup>38</sup>

Because the actual conditions are not the same as the ideal combustion conditions, excessive air is used to ensure complete combustion. Excessive air use can be considered as a measure against the risk of flame failure or explosion as a consequence of insufficient oxygen. The excess air avoids unused fuel, ensures stable combustion and prevents the formation of carbon monoxide, a toxic gas.

### 2.3.2. Flame Types

#### 2.3.2.1. Premixed Flames

Premixed flames occur when the fuel and air quantities are sent at the desired rates before entering the burner. The premix makes it possible to achieve a uniform flame.<sup>39</sup>

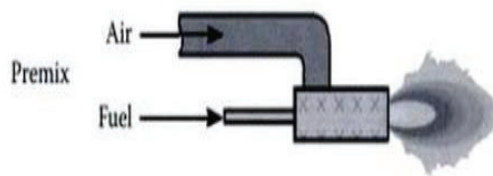


Figure 2.2. Premixed Flame<sup>40</sup>

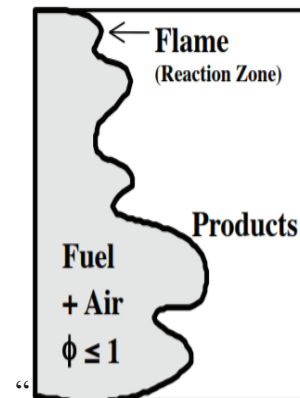


Figure 2.3. Schematic view of Premixed Flame<sup>41</sup>

The flame speed depends on the type of fuel, the mixing ratio, and the mixing temperature. For controlled combustion, the rate of arrival of the mixture must be somewhat higher than the flame speed.<sup>42</sup>

If the rate of arrival of the mixture is greater than the flame speed, the flame breaks off at the burning end and extinguishes. It's called a flame break. If the arrival rate of the mixture is less than the flame speed, then the flame spreads into the mixing channel. This is called flame inward thrust.<sup>42</sup>

Examples of premixed laminar flames include Bunsen flames, and pre-mixed turbulent flames are examples of gasoline engines. Compared to other flame types, the mixture ratio and combustion process can be controlled more easily in premixed flames.<sup>42</sup>

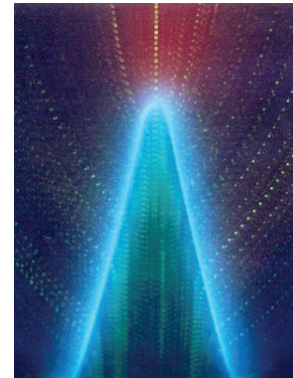


Figure 2.4. Bunsen Burner  
Methane-Air  
Premixed Flame<sup>41</sup>

### 2.3.2.2. Diffusion (Non-Premixed) Flames

In diffusion-type flames, the fuel comes to the burner alone and the burning fuels become the area where air circulates around.<sup>42</sup>

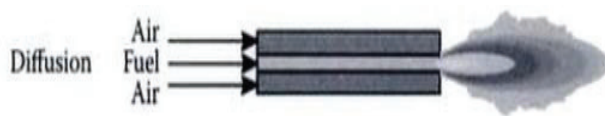


Figure 2.5. Diffusion Flame<sup>40</sup>

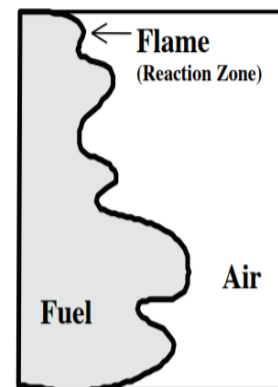


Figure 2.6. Schematic view of  
Diffusion Flame<sup>41</sup>

In the diffusive flames, there is almost no air on the near side of the mixing zone, whereas on the air side the fuel ratio approaches zero. The intense flame and brightness are in the stoichiometric region ( $\phi = 1$ ).<sup>42</sup>

Uniformity of the air-fuel mixture in the formation of diffusion flames results in the formation of unburned carbon particles (soot).<sup>42</sup>

Examples of pre-mixed laminar flames include candle flame, pre-mixed turbulent flames, and the most commonly used flame in industrial furnaces and jet fuels.<sup>42</sup>

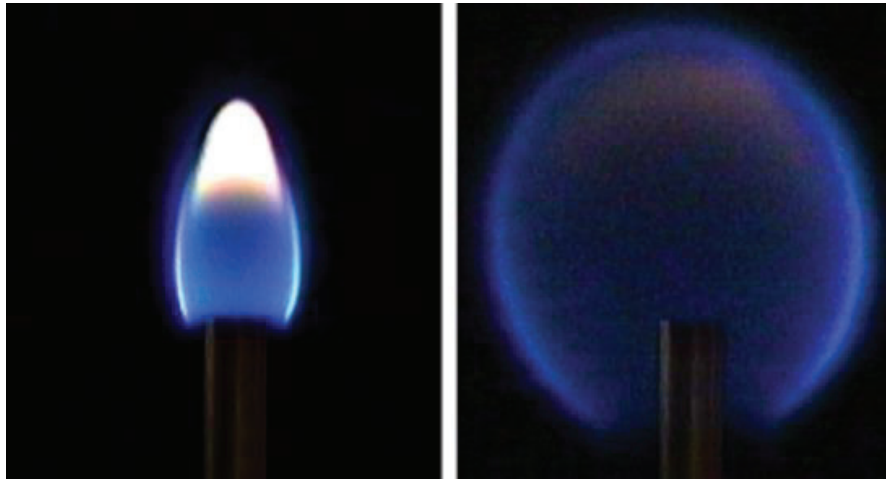


Figure 2.7. Examples of Diffusion Type Jet Fuels<sup>41</sup>

### 2.3.2.3. Partially Premixed Flames

Partially premixed flames are flame types in which fuel and air are premixed at unequal rates.<sup>39</sup>

In the case of premixed or diffusion flame types, precise mixing of fuel and air is a little difficult under real conditions. In practical applications, partially premixed flame types have more common usage.<sup>43</sup>

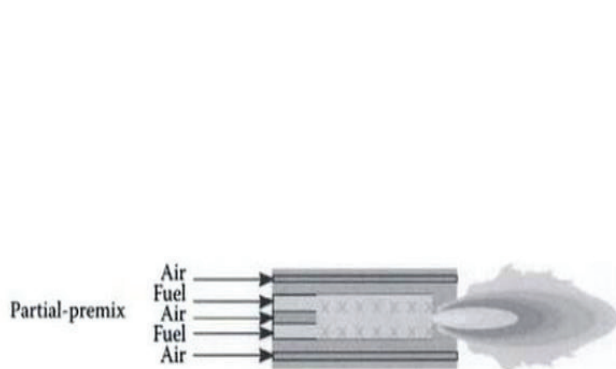


Figure 2.8. Partial Premixed Flame<sup>40</sup>

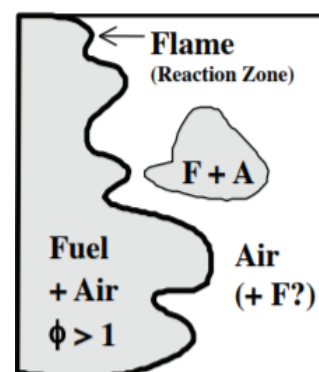


Figure 2.9. Schematic view of Partial Premixed Flame<sup>41</sup>

## 2.3.2 Combustion Equations

As mentioned earlier, oxidation of the fuel is necessary for the combustion to take place. Air is often used instead of pure oxygen for this reaction.

Knowing the oxygen content in the air is very important to form the combustion equations. As is known, the air is largely composed of Nitrogen (78%) and Oxygen (21) atoms. Argon with 0.9% of the largest component of the remaining 1%. All other gases in the air are as low as 0.1% in total. These ratios are shown in Figure 2.10.

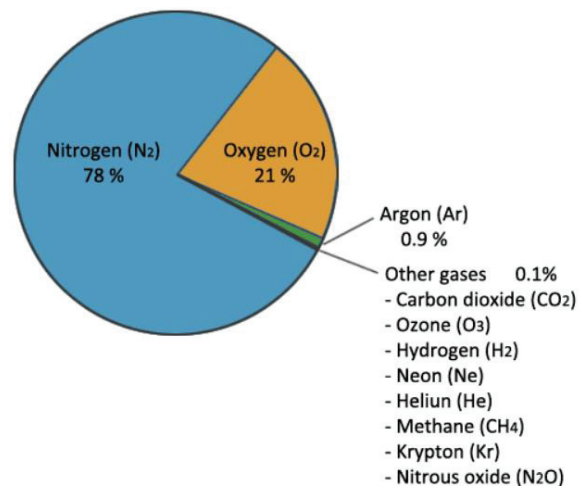


Figure 2.10. Composition of Air<sup>44</sup>

The elements which are the total of 0.1% in the air and their presence ratio in the air are shown in the following figure.

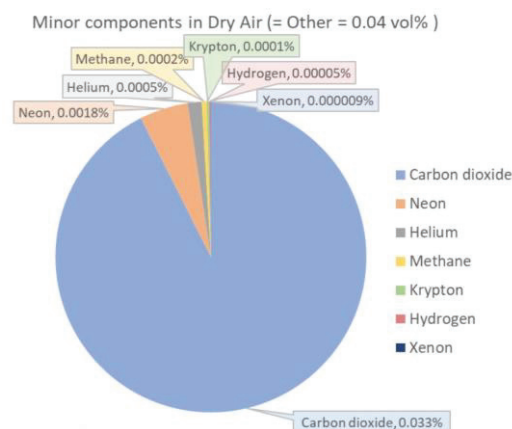


Figure 2.11. Minor Components in Dry Air<sup>45</sup>

Combustion in the combi boilers takes place in the combustion chamber. The combustion in the condensing combi boiler occurs in the exchanger, while the combustion in the conventional combi boiler takes place in the combustion chamber under the primary heat exchanger.

In the combi boilers, natural gas is usually used as a fuel. Natural gas is made up substantially of methane. Because of this, in the equations methane is used as a fuel in generally showing the combustion equation of natural gas, while air components ratios are taken approximately as 20% oxygen and 80% nitrogen.

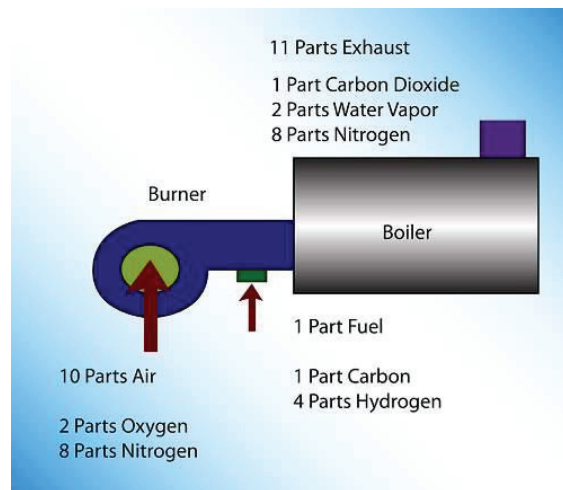


Figure 2.12. Basic Combustion Reactions<sup>46</sup>

In real life, natural gas does not consist of just methane. In order to make scientific calculations, it is first necessary to examine the content of the natural gas and to know exactly the components of the contents.

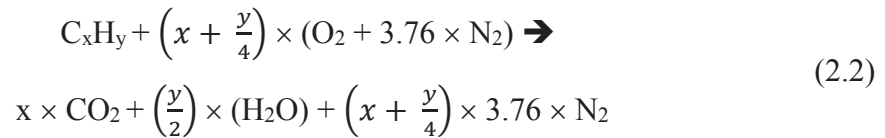
Although natural gas is predominantly methane, it also contains different hydrocarbon groups. It also contains nitrogen, carbon monoxide, oxygen, and hydrogen, even in small quantities. These components and component ratios are given in table 2.1.

When these components are considered, the fuel is shown as  $\text{C}_x\text{H}_y$ . Where  $x$  symbol represents the number of carbon atoms in the fuel, and  $y$  symbol represents the number of hydrogen atoms in the fuel. In addition, for the theoretical air that is included in the equation, the components in the low air content are neglected and the component ratio is calculated as 21% oxygen and 79% nitrogen.

Table 2.1. Components of the Natural Gas<sup>47</sup>

Component	Symbol	Typical Analysis (Mole %)	Range (Mole %)
Methane	CH <sub>4</sub>	93.9	87.0 - 97.0
Ethane	C <sub>2</sub> H <sub>6</sub>	4.2	1.5 - 9.0
Propane	C <sub>3</sub> H <sub>8</sub>	0.3	0.1 - 1.5
Butane	C <sub>4</sub> H <sub>10</sub>	0.06	0.01 - 0.3
Pentane	C <sub>5</sub> H <sub>12</sub>	0.02	trace - 0.04
Hexanes plus	C <sub>6</sub> H <sub>14</sub>	0.01	trace - 0.06
Nitrogen	N <sub>2</sub>	1.0	0.2 - 5.5
“Carbon Dioxide	CO <sub>2</sub>	0.5	0.05 - 1.0
Oxygen	O <sub>2</sub>	0.01	trace - 0.1
Hydrogen	H	trace	trace - 0.02

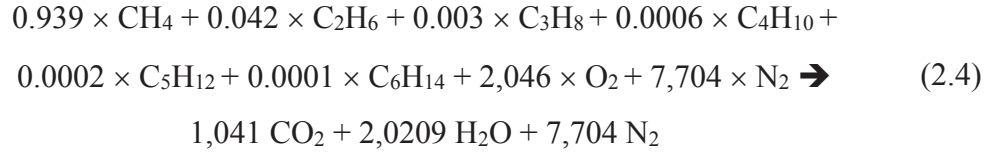
In the light of all of this information and negligible values, the combustion equation used in theory can be shown as in equation 2.2.



If natural gas is used as the test gas, the equations evolves as follows:

$$\begin{aligned}
&0.939 \times CH_4 + 0.939 \times (2) \times (O_2 + 3.76 \times N_2) + 0.042 \times C_2H_6 + 0.042 \\
&\times (3.5) \times (O_2 + 3.76 \times N_2) + 0.003 \times C_3H_8 + 0.003 \times (5) \times (O_2 + 3.76 \\
&\times N_2) + 0.0006 \times C_4H_{10} + 0.0006 \times (6.5) \times (O_2 + 3.76 \times N_2) + 0.0002 \\
&\times C_5H_{12} + 0.0002 \times (8) \times (O_2 + 3.76 \times N_2) + 0.0001 \times C_6H_{14} + 0.0001 \\
&\times (9.5) \times (O_2 + 3.76 \times N_2) + 0.01 \times N_2 + 0.005 \times CO_2 \rightarrow \\
&0.939 \times CO_2 + 0.939 \times (2) \times (H_2O) + 0.939 \times (2) \times 3.76 \times N_2 + 0.042 \\
&\times 2 \times CO_2 + 0.042 \times (3) \times (H_2O) + 0.042 \times (3.5) \times 3.76 \times N_2 + 0.003 \\
&\times 3 \times CO_2 + 0.003 \times (4) \times (H_2O) + 0.003 \times (5) \times 3.76 \times N_2 + 0.0006 \times \\
&4 \times CO_2 + 0.0006 \times (5) \times (H_2O) + 0.0006 \times (6.5) \times 3.76 \times N_2 + \\
&0.0002 \times 5 \times CO_2 + 0.0002 \times (6) \times (H_2O) + 0.0002 \times (8) \times 3.76 \times N_2 + \\
&0.0001 \times 6 \times CO_2 + 0.0001 \times (7) \times (H_2O) + 0.0001 \times (9.5) \times 3.76 \times N_2 \\
&+ 0.01 \times N_2 + 0.005 \times CO_2
\end{aligned} \quad (2.3)$$

When we edit the equation:

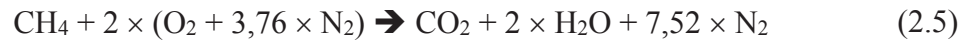


The tests were performed by using G20 gas. The composition of test reference gases, including G20 gas, are given in table 2.2.

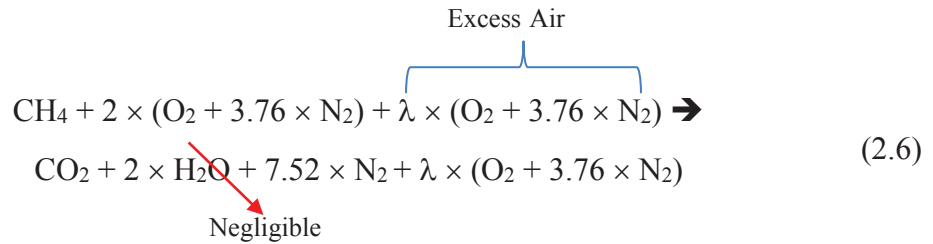
Table 2.2. Composition of Test Reference Gases<sup>48</sup>

Composition		Test Reference Gas			
		G <sub>20</sub>	G <sub>23</sub>	G <sub>25</sub>	G <sub>R</sub>
Methane C <sub>1</sub>	%mol	99.5 ± 0.5	92.5 ± 1	86 ± 2	87 ± 2
Ethane C <sub>2</sub>	%mol	-	-	-	13 ± 2
Balance	%mol Max	1	1	1	1
N <sub>2</sub>	%mol	-	7.5 ± 1	14 ± 2	-
S	mg/kg Max	10	10	10	10
W.I.	Nr (LHV)	48 ± 0.2	44 ± 0.5	41.5 ± 1	48.5 ± 0.5
MN	Nr	95 - 100	82 - 85	70 - 76	70 - 78
MON	Nr	137-140	128-130	120-124	120-126

The content of G20 gas consists of 100% methane gas (CH<sub>4</sub>) when the tolerance value is also considered. In this case, a simpler equation appears as shown below.



During actual combustion, some excess air enters the combustion chamber. This equation can be shown as follows. ("λ" refers to excess air ratio in the equation)



In order to find the value of λ in the equation, the mapping test results which will be mentioned in the next section are used.

## 2.4 Condensation

Condensation is state of the gas molecules passes through the liquid phase. Condensation is observed as the result of the gas molecules begin to move slowly enough to become liquid with the loss of energy. This usually happens with the result of the gas molecules losing their energy and striking a cold surface. After the end of this collision, liquefaction occurs.

The water vapor in the air is composed of  $\text{H}_2\text{O}$  molecules with a certain kinetic energy. Normally, due to this kinetic energy,  $\text{H}_2\text{O}$  molecules don't adhere to each other and do not form liquid water droplets. But these molecules can form liquid water droplets by giving their temperature when their atoms hit a cooler surface than the temperature of the water vapor, or they transmit their kinetic energy to this hitting surface.

When one of these conditions occurs, if water vapor stays on the surface it is called adsorption. The rapidity of the process depends on the surface coldness and the presence of dissolved water molecules in the air. In such cases, the cooling occurrence is faster than evaporating the water by air. In the case of dry air, the occurrence of the evaporation of the water is faster than the occurrence of the accumulated water on the surface result of the cooling.

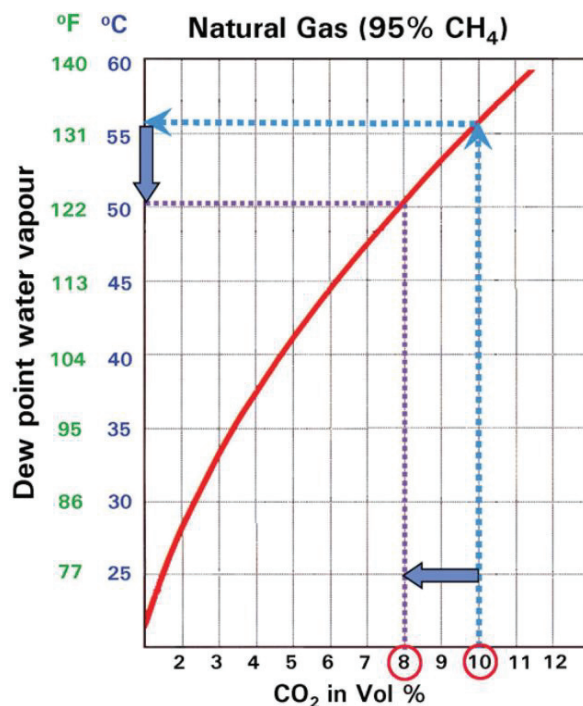


Figure 2.13. CO<sub>2</sub> in vol % - Dew Point Water Vapor Graph for Natural Gas<sup>49</sup>



The dew point temperature values corresponding to the CO<sub>2</sub> ratios found in the graph in the Figure 2.13 are found and those values shown in table 2.3.

Table 2.3. Dew Point Water Vapor Values Corresponding to CO<sub>2</sub> in vol %

CO <sub>2</sub> (%)	1%	1,50%	2%	2,50%
Temperature (°C)	22 °C	25 °C	28,4 °C	30,6 °C
CO <sub>2</sub> (%)	3%	3,50%	4%	4,50%
Temperature (°C)	33,8 °C	35,2 °C	37,4 °C	39,8 °C
CO <sub>2</sub> (%)	5%	5,50%	6%	6,50%
Temperature (°C)	42 °C	43,5 °C	44,3 °C	46,5 °C
CO <sub>2</sub> (%)	7%	7,50%	8%	8,50%
Temperature (°C)	47,4 °C	49 °C	50 °C	52,2 °C
CO <sub>2</sub> (%)	9%	9,50%	10%	10,50%
Temperature (°C)	53,1 °C	54,5 °C	55,9 °C	57,3 °C
CO <sub>2</sub> (%)	11%	11,50%		
Temperature (°C)	58,2 °C	59,4 °C		

## CHAPTER 3

### TEST RESULTS & CALCULATIONS

#### 3.1. Mapping Test Method

In the mapping tests, the percent CO<sub>2</sub> rate, the exhaust gas temperatures at that region, approximately efficiency and excess air rates and the amount of CO, O<sub>2</sub>, NO, NO<sub>x</sub>, etc. as the ppm values are measured at the most common inlet-outlet water temperatures for cases where the appliance is operating at minimum or maximum burner pressure. The percentage of CO<sub>2</sub> results from these measurements can be used to determine how well the appliance has performed the combustion process in reference to the theoretical combustion equation.

Mapping tests are important in terms of knowing the amount of CO and the regions in which these quantities are concentrated. As it is known, it is important to keep the CO that is dangerous for health in a safe boundary. In order to take precautions for zones with high values on a particle basis, mapping scanning is important.

In the mapping tests, the part that interests us in terms of condensation is CO<sub>2</sub> percentages and temperature distributions over the HEx. As indicated in the graph in the Figure 2.13, CO<sub>2</sub> concentration in the flue gas determines the point of condensation. The temperature distribution over the exchanger also helps us to find the pipe surface temperature in that area. For the condensation to take place, the temperature of the dew point in that area must be higher than the pipe surface temperature. In this condition, the water vapor in the flue gas will strike a cooler surface than itself and leave its heat and will transition to liquid form.

The important thing to avoid from condensation is to reduce the CO<sub>2</sub> rate and to draw down the condensation point. At the same time, if the pipe surface temperature through those areas can be stayed on over the dew point, the condensation situation can be prevented. In this way, negative conditions such as copper corrosion, soot formation and the decrease of the appliance's efficiency can be eliminated as well. With this tests, it is possible to determine the risky regions where the condensation can be seen.

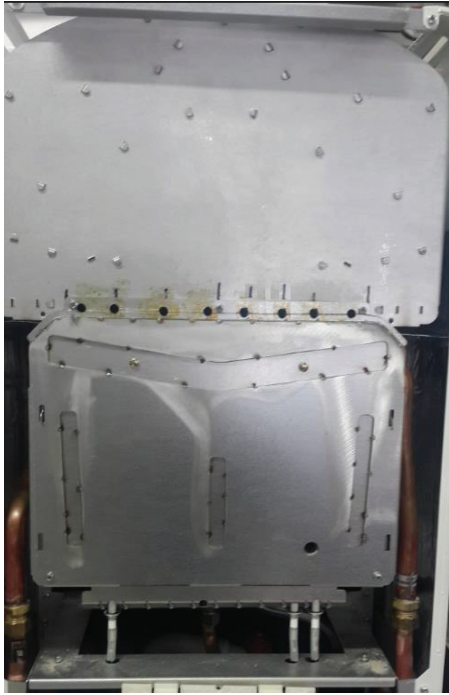


Figure 3.1. Unscrewed front panel of the B type conventional appliance

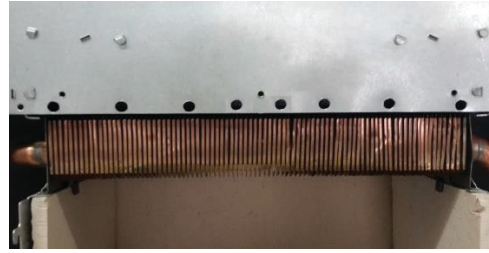


Figure 3.2. Points of the drilling in a hole on the surface for B type appliance

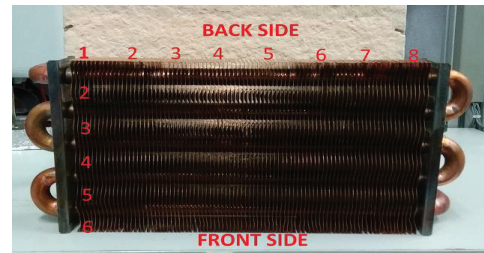


Figure 3.3. Mapping points on the Cu HEx for B type appliance



Figure 3.4. Unscrewed front panel of the C type conventional appliance

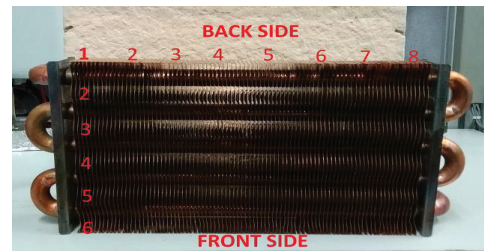


Figure 3.5. Mapping points on the Cu HEx for C type appliance

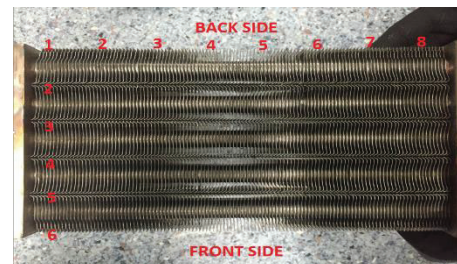


Figure 3.6. Mapping points on the SS HEx for C type appliance

After unscrewed the front panel of the appliance which was hanged on the test stand, holes were drilled into the combustion chamber lid evenly along the heat exchanger line. It was paid attention that these holes were as large as the measuring probe could pass through. For cases where the appliance is operating at minimum or maximum burner pressure, the CO<sub>2</sub> percentages, and the exhaust gas temperatures in that region were measured at the most common inlet-outlet water temperature. The percentage of carbon dioxide in the exhaust gas is the first step to find out how close the appliance is to the condensation situation. Our first purpose in this study is to find the critical dew point temperatures by positioning in the graph the percentage of CO<sub>2</sub> coming from the mapping test.

In the mapping test results, temperature values, carbon monoxide particle numbers or carbon dioxide ratios are high at some points because of the flame profile on the burner is not uniform. The factors affecting this situation are the fan position in C type conventional appliances and the non-uniform air flow under the influence of draught diverter over the combustion chamber in B type conventional appliances. In C type conventional combi boiler appliances, the fan of the appliance is mounted on just one side where either the right or left side of the fan hood area. This affects the uniform distribution of airflow. In condensing combi boiler appliances, heat is generated inside the heat cell. Thanks to the premix unit in this type of appliance, the air-fuel mixture is prepared before entering the heat cell, so a homogeneous mixture and uniform combustion are observed in the heat cell.

Mapping tests were first carried out on the conventional appliance of Type B and Type C using the same copper heat exchanger. As mentioned earlier, type B has a natural flow, in the case of type C has a forced flow through a fan. This affects the amount of fresh air entering combustion equations. Combustion equations in two cases contain excess air quantity at different rates. This affects combustion products. CO<sub>2</sub> and temperature distributions in the flue gas area are changing because of the amount of excess air changes in the same heat exchanger design parameters. In this case, the critical dew points also vary. In the mapping tests, the results for B type and C type appliances with copper heat exchanger were given as 47/53°C for min load and 60/80°C for max load. In first section, the effect of the combustion equations on the condensation state is observed.

In the results to be interpreted on the following pages, after changed the material and parameters of the heat exchanger, the test results were given for C type appliances with stainless steel heat exchanger. For this appliance's mapping test, only sharing the max load 60/80°C results were considered enough. In this second part, the effect of changes in the design parameters targeted throughout the thesis is observed.

Table 3.1 shows the geometric parameter variables for the heat exchangers which is manufactured from fin material Cu – DHP and fin material SS – 1.4509.

Table 3.1. Specifications of Material Parameters

	Parameter	Cu - DHP	SS - 1.4509	Unit
<b>Thermal Conductivities of Materials</b>	Fin	339	25	W/m•K
	Pipe	339	339	W/m•K
<b>Geometric Dimensions of Fin</b>	Length	$182.2 \times 10^{-3}$	$192.1 \times 10^{-3}$	m
	Height	$45 \times 10^{-3}$	$52 \times 10^{-3}$	m
	Thickness	$0.35 \times 10^{-3}$	$0.42 \times 10^{-3}$	m
	Pitch	$2.35 \times 10^{-3}$	$2.1 \times 10^{-3}$	m
<b>Fin Number</b>		88	115	
<b>Geometric Dimensions of Pipe</b>	Length	$268 \times 10^{-3}$	$293.5 \times 10^{-3}$	m
	Outside Diameter	$20.9 \times 10^{-3}$	$26.6 \times 10^{-3}$	m
	Thickness	$0.75 \times 10^{-3}$	$0.80 \times 10^{-3}$	m

## 3.2. Test Results and Calculations

### 3.2.1. Mapping Results at Min Load & Calculations

When making tests for the condensation, the tests were first carried out under the min load condition. The reason for choosing 47/53°C in the shared data of these tests made according to the standards is having high CO<sub>2</sub> ratios and low-temperature distributions compared to other min load tests.

In the following tables and graphs, the percent of the carbon dioxide rate and flue gas temperature distribution are given for the **copper** heat exchanger of the **B type conventional appliance**.

Table 3.2. %CO<sub>2</sub> rate distribution over the B type Cu HEx at min load (47/53°C)

MIN 47/53°C							
Back side of heat exchanger							
CO <sub>2</sub> (%)							
1,85	2,54	1,91	1,68	1,75	1,63	1,58	1,47
2,45	2,91	2,69	2,57	2,88	2,47	2,64	2,52
2,71	2,57	2,61	2,72	2,91	2,74	2,80	2,71
2,59	2,21	2,19	2,41	2,23	2,39	2,64	2,52
2,11	2,32	3,00	2,42	2,88	2,61	2,34	2,44
2,09	2,75	2,77	2,52	2,81	2,67	2,57	2,48
front side of heat exchanger							

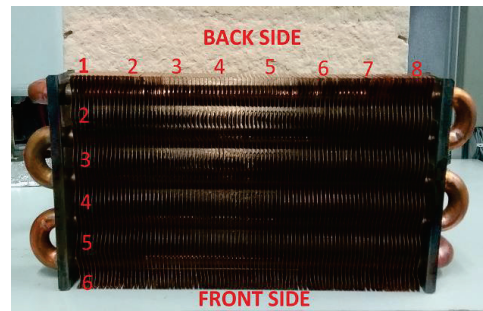


Figure 3.3. Mapping points on the Cu HEx

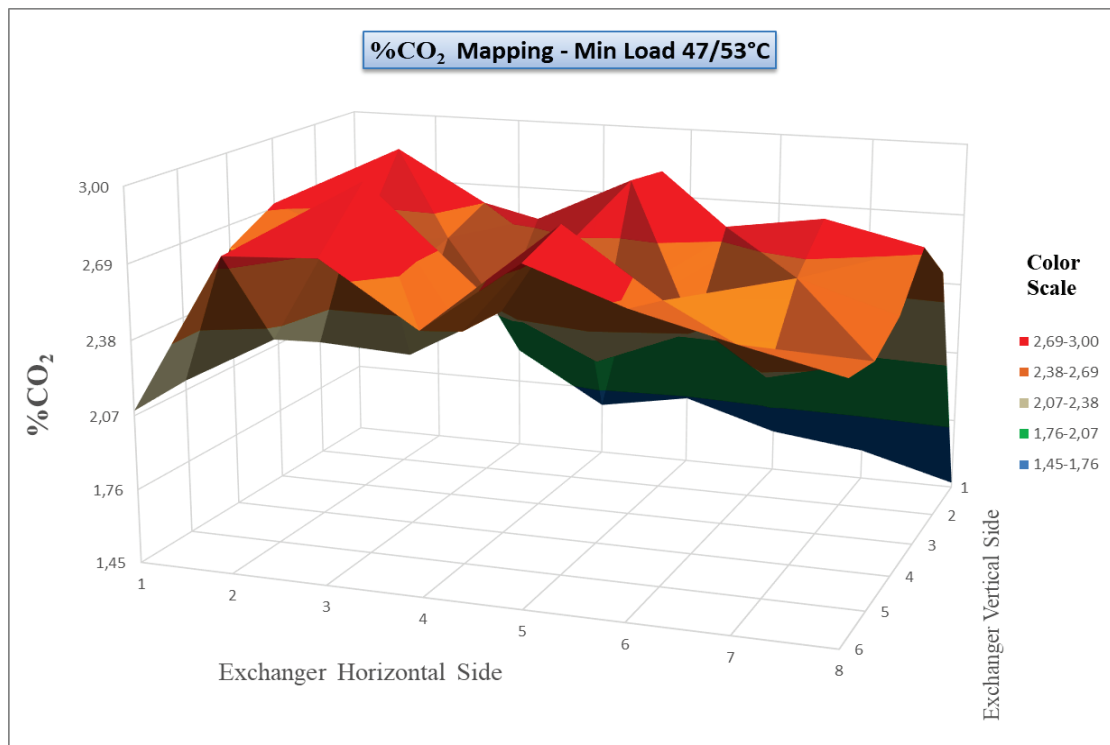
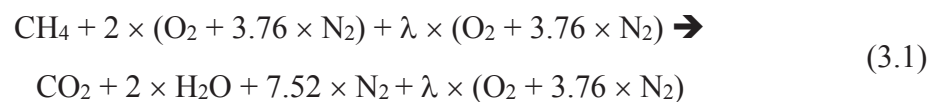


Figure 3.7. %CO<sub>2</sub> rate distribution over the Cu HEx at min load (47/53°C) for B type appliance

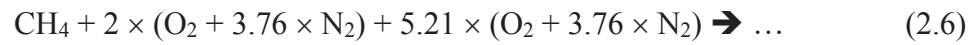
Besides finding the critical dew point temperature, the CO<sub>2</sub> ratio allows us to find N<sub>2</sub> and O<sub>2</sub> in the flue gas using Equation 2.6, to use them in the heat transfer calculations to be done for the air side.





The critical point was defined as the EVS 5 X EHS 3 point over the heat exchanger where both **low temperature (66.9°C)** and the **high CO<sub>2</sub> (%3.00)** rate as a result of the measurements made under the stated operating conditions. According to the calculations made using **CO<sub>2</sub> ratio 3.00%** and using equation 2.6, the excess air amount  $\lambda = 5.21$ , the **N<sub>2</sub>** and **O<sub>2</sub>** ratios in the flue gas in this region is **81.36%** and **15.63%** respectively. These values serve us to calculate the Prandtl, viscosity, density and thermal conductivity to be used for the heat transfer of airside. The sum of **CO<sub>2</sub>**, **N<sub>2</sub>** and **O<sub>2</sub>** ratios is **99.99%**.

Once we had calculated excess air quantity ( $\lambda$ ), we had also been able to calculate how much air will be required for 1 m<sup>3</sup> CH<sub>4</sub>.



$$\text{For } 1 \text{ m}^3 \text{ CH}_4 \rightarrow 7.21 \text{ m}^3 \text{ O}_2 + 27.12 \text{ m}^3 \text{ N}_2 = 34.33 \text{ m}^3 \text{ air is required.} \quad (3.2)$$

In order to find the air flow rate when the appliance performs combustion during the tests, it is first necessary to find the amount of gas that is burned during the test. Although the amount of gas used can be taken from the test rig data during the tests, it is also possible to make the approximate calculation by a simple method. So, when you want to make calculations without testing, you can calculate the amount of gas that goes through this way.

For this, firstly the heat input ( $Q_i$ ) of the appliance is calculated. After then, the gas flow rate is calculated using the net calorific value ( $H_i$ ) of the gas.

To calculate the heat input with a simple method:

$$Q_i = \frac{Q_o}{\eta_a} \quad (3.3)$$

The appliances used in the tests are 2-star category appliances. For a 2 star 24 kW appliance, efficiency should be  $\geq 89.76 \%$ .

For min load measurement:  $Q_o = 8 \text{ kW}$

$$\text{So; } Q_i = 8.91 \text{ kW} \quad (3.4)$$

For gas flow rate; ( $H_i=34.02 \text{ MJ/m}^3$  for G20)

$$\dot{V}_g = \frac{Q_i}{H_i} = 0.94 \text{ m}^3/\text{h} \quad (3.5)$$

The heat input ( $Q_i$ ) is calculated by the program in the test rig using the following formula.

$$Q_i = H_i \times \frac{10^3}{3600} \times \dot{V}_g \times \sqrt{\frac{1013.25 + p_g}{1013.25} \times \frac{p_a + p_g}{1013.25} \times \frac{288.15}{273.15 + t_g} \times \frac{d}{d_r}} \quad (3.6)$$

From the test rig data it is seen that the gas amount ( $v_g$ ) is  $0.98 \text{ m}^3/\text{h}$  and the heat input ( $Q_i$ ) from its calculations is  $9 \text{ kW}$ .

As can be seen from the differences between the calculations, there is a deviation of 4% in gas flow rate ( $\dot{V}_g$ ) and 1% in heat input ( $Q_i$ ). These deviations, which are not more than 5%, can be ignored and calculations methods in equation 3.4 and 3.5 can be used instead of test rig data from the performed test.

In equation 3.2 we found that  $34.33 \text{ m}^3$  of fresh air is needed for  $1 \text{ m}^3$  of  $\text{CH}_4$  gas. In equation 3.5, we calculated that the appliance consumes a total of  $0.94 \text{ m}^3/\text{h}$  gas during the tests. From here;

For  $0.94 \text{ m}^3/\text{h}$  test gas  $\rightarrow 32.38 \text{ m}^3/\text{h}$  fresh air is used during the test which performed under the stated operating conditions.

Table 3.3. Temperature distribution over the B type Cu HEX at min load (47/53°C)

MIN 47/53°C							
Back side of heat exchanger							
Temperature (°C)							
65,9	70,2	71,5	74,4	69,8	73,1	74,2	68,8
67,7	70,9	74,4	71,1	73,3	68,8	64,7	58,9
69,1	73,2	71,4	68,5	73,4	69,9	70,1	61,8
66,3	70,1	67,7	69,1	70,3	62,8	61,4	59,9
59,8	63,4	66,9	68,1	66,2	63,7	63,3	60,1
61,2	71,1	70,8	72,1	73,4	68,7	66,6	63,7
front side of heat exchanger							

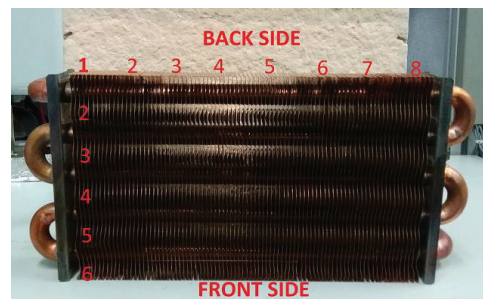


Figure 3.3. Mapping points on the Cu HEX



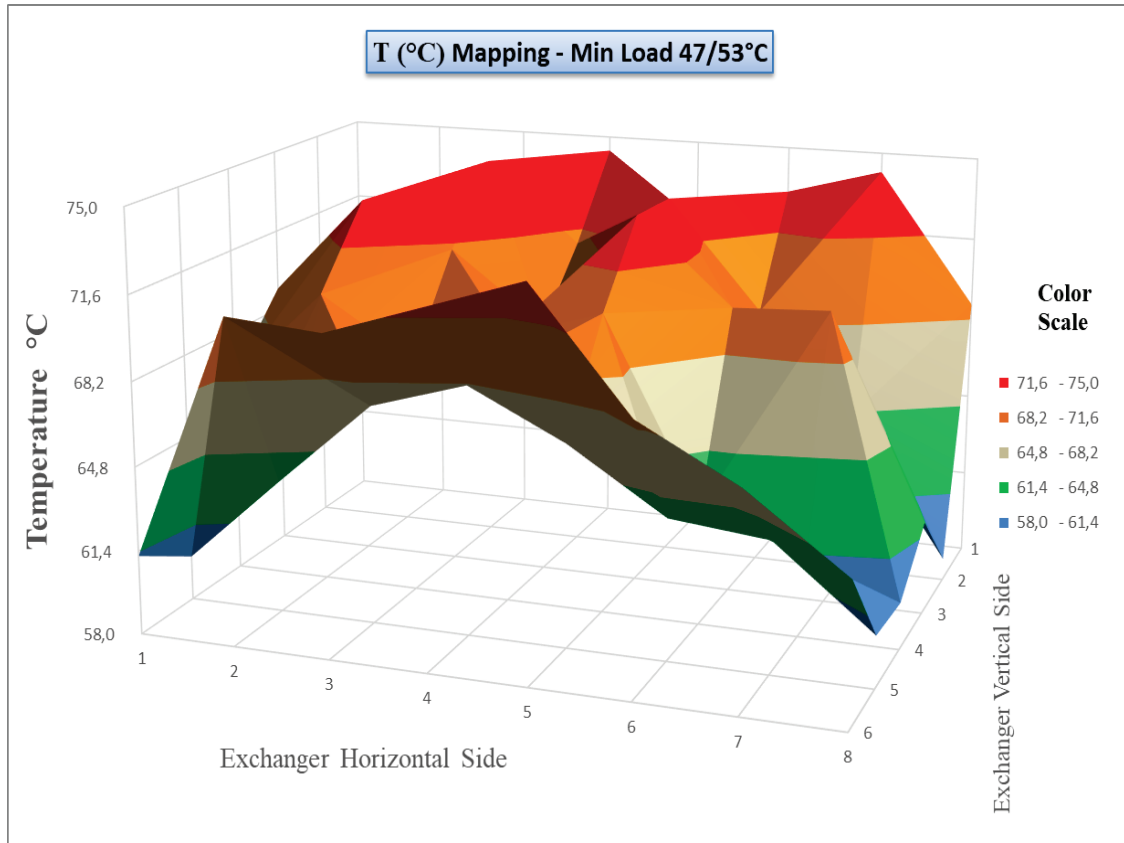


Figure 3.8. Temperature distribution over the Cu HEx at min load (47/53°C) for B type appliance

The temperature distribution values from the mapping test are used to find the regional pipe outer surface temperatures on the heat exchanger. For this, firstly heat transfer coefficients are calculated for both flue gas and water sides.

First of all, density, viscosity, Prandtl number and thermal conductivity values of CO<sub>2</sub>, N<sub>2</sub>, and O<sub>2</sub> were taken from the thermophysical properties table<sup>5</sup> in order to calculate those values of the flue gas side.

The thermophysical properties values of CO<sub>2</sub>, N<sub>2</sub>, and O<sub>2</sub> for 147°C are given in Table 3.4. In the beginning, 650°C which is the combustion gas temperature for natural gas was taken as the starting point.<sup>50</sup> It is because the appliance works at minimum load in 47/53°C tests, 220°C was taken instead of 650°C. As a result of the iterations, combustion gas temperature was found and 147°C was obtained by taking the average with the flue gas temperature. As the reason for the low-temperature value under the heat exchanger, it can be said that the appliance consumes low fuel under minimum load condition.

Table 3.4. Thermophysical properties of CO<sub>2</sub>, N<sub>2</sub> and O<sub>2</sub> at 147°C<sup>5</sup>

<b>T<sub>fga</sub></b>	<b>Average flue gas temperature</b>	147	°C
<b>Pr<sub>N2</sub></b>	<b>Prandtl number of N<sub>2</sub></b>	0.704	
<b>Pr<sub>CO2</sub></b>	<b>Prandtl number of CO<sub>2</sub></b>	0.735	
<b>Pr<sub>O2</sub></b>	<b>Prandtl number of O<sub>2</sub></b>	0.738	
<b>k<sub>N2</sub></b>	<b>Thermal conductivity of N<sub>2</sub></b>	34×10 <sup>-3</sup>	W/m•K
<b>k<sub>CO2</sub></b>	<b>Thermal conductivity of CO<sub>2</sub></b>	25.1×10 <sup>-3</sup>	W/m•K
<b>k<sub>O2</sub></b>	<b>Thermal conductivity of O<sub>2</sub></b>	33.7×10 <sup>-3</sup>	W/m•K
<b>ρ<sub>N2</sub></b>	<b>Density of N<sub>2</sub></b>	0.812	kg/m <sup>3</sup>
<b>ρ<sub>CO2</sub></b>	<b>Density of CO<sub>2</sub></b>	1.275	kg/m <sup>3</sup>
<b>ρ<sub>O2</sub></b>	<b>Density of O<sub>2</sub></b>	0.940	kg/m <sup>3</sup>
<b>μ<sub>N2</sub></b>	<b>Viscosity of N<sub>2</sub></b>	2.28×10 <sup>-5</sup>	N•s/m <sup>2</sup>
<b>μ<sub>CO2</sub></b>	<b>Viscosity of CO<sub>2</sub></b>	1.98×10 <sup>-5</sup>	N•s/m <sup>2</sup>
<b>μ<sub>O2</sub></b>	<b>Viscosity of O<sub>2</sub></b>	2.67×10 <sup>-5</sup>	N•s/m <sup>2</sup>

After these values are found, density, viscosity, Prandtl number and thermal conductivity values of the flue gas side are calculated by multiplying the ratios of CO<sub>2</sub>, N<sub>2</sub>, and O<sub>2</sub> in the flue gas. The values in Table 3.4 were multiplied by the CO<sub>2</sub>, N<sub>2</sub> and O<sub>2</sub> ratios in the flue gas and thus the flue gas values in Table 3.5 were calculated.

Table 3.5. Thermophysical properties of Flue gas for the B type Cu HEx at min load (47/53°C)

<b>Flue gas content (N<sub>2</sub> + CO<sub>2</sub> + O<sub>2</sub>) = 0.99</b>	0.813	0.030	0.156
<b>Pr<sub>fg</sub></b>	<b>Prandtl number of flue gas</b>	0.7102	
<b>k<sub>fg</sub></b>	<b>Thermal conductivity of flue gas</b>	33.6×10 <sup>-3</sup>	W/m•K
<b>ρ<sub>fg</sub></b>	<b>Density of flue gas</b>	0.845	kg/m <sup>3</sup>
<b>μ<sub>fg</sub></b>	<b>Viscosity of flue gas</b>	2.32×10 <sup>-5</sup>	N•s/m <sup>2</sup>

Other unknowns required to calculate the Re number on the gas side are the gas velocity and the gas side hydraulic diameter.

The following formula is used when calculating the speed.

$$\dot{V}_{fg} = v_{fg} \times A_{gfa} \quad (3.7)$$

Using Equation 3.5 and 3.2 we found the gas and the fresh air flow rate to be 0.94 m<sup>3</sup>/h and 32.38 m<sup>3</sup>/h. To calculate the flue gas velocity, this value is converted to m<sup>3</sup>/s and the hydraulic diameter value for Cu HEX is found and necessary calculations are made. Table 3.6 shows the calculation parameters for Re and Nu numbers.

Table 3.6. Calculation parameters for Re and Nu numbers of Flue Gas side for the B type Cu HEX at min load (47/53°C)

<b>Flue Gas Side - Cu HEX</b>				
<b><math>\dot{V}_{fg}</math></b>	<b>Gas flow rate (G20)</b>	33.32	m <sup>3</sup> /h	0.0093 m <sup>3</sup> /s
<b><math>A_{fg}</math></b>	<b>Gas flow area</b>	0.018	m <sup>2</sup>	
<b><math>v_g</math></b>	<b>Gas velocity</b>	0.51	m/s	
<b><math>Dh_{Cu}</math></b>	<b>Hydraulic diameter of Cu HEX</b>	1.86	mm	0.00186 m
<b><math>Y</math></b>	<b>Fin pitch</b>	$2.35 \times 10^{-3}$	m	
<b><math>H</math></b>	<b>Fin height</b>	0.045	m	
<b><math>\delta_f</math></b>	<b>Fin thickness (tr)</b>	$35 \times 10^{-5}$	m	

The Reynolds number, Nusselt numbers and the heat transfer coefficient of the flue gas side are calculated by the following formulas in the light of the information in the tables.

For Reynolds Number on Air Side;

$$Re_{fg} = \frac{\rho_{fg} \times v_{fg} \times Dh_{Cu}}{\mu_{fg}} = 34.26 \quad (3.8)$$

For Nusselt Number on Air Side;

$$Nu_{fg} = 0.1507 \times Re^{0.667} \times Pr^{1/3} \times \left(\frac{Y}{H}\right)^{0.164} \times \left(\frac{Y}{\delta_{fin}}\right)^{0.075} = 1.009 \quad (3.9)$$

For Heat Transfer Coefficient on Flue Gas Side;

$$h_{fg} = \frac{Nu_{fg} \times k_{fg}}{Dh_{fg}} = 18.28 \text{ W/m}^2 \cdot \text{K} \quad (3.10)$$

To find the heat transfer coefficient for the water, the exchanger parameters in Table 3.7 were used. Due to exchanger parameters, water velocity and hydraulic diameter are calculated.

Table 3.7. Heat Exchanger Design Parameters for Cu HEx

<b>Parameters for Cu HEx</b>				
<b>L<sub>p</sub> pipe length</b>	1340	mm	1.34	m
<b>D<sub>2</sub> outer diameter of pipe</b>	20.9	mm	0.0209	m
<b>D<sub>1</sub> inner diameter of pipe</b>	20.15	mm	0.02015	m
<b>r<sub>2</sub> outer pipe radius</b>	10.45	mm	0.01045	m
<b>r<sub>1</sub> inner pipe radius</b>	10.075	mm	0.010075	m
<b>t<sub>p</sub> thickness of pipe</b>	0.75	mm	0.00075	m
<b>A<sub>p</sub> pipe area</b>	318.89	mm <sup>2</sup>	0.00032	m <sup>2</sup>
<b>S<sub>p</sub> surface of pipe</b>	63.30	mm	0.06330	m

The following formula is used when calculating the speed.

$$\dot{V}_w = v_w \times A_p \quad (3.11)$$

To calculate the water velocity, water flow rate value is converted to m<sup>3</sup>/s and the hydraulic diameter value for water side is found and necessary calculations are made. Table 3.8 shows the calculation parameters for Re and Nu numbers.

Table 3.8. Calculation parameters for Re and Nu numbers for Cu HEx

<b><math>\dot{V}_w</math> (Flow rate)</b>	18	l/min	0.0003	m <sup>3</sup> /s
<b>v<sub>w</sub> (water velocity)</b>	0.940	m/s		
<b>Dh<sub>w</sub> (Hydraulic diameter)</b>	0.02015	m		

Table 3.9 shows the thermophysical properties such as density, viscosity, Prandtl number and thermal conductivity values at 50°C, which is the average temperature for water 47/53°C tests. In the beginning, 50°C which is the average value for 47/53°C tests

was taken as the starting point. As a result of the iterations, the average water temperature was found nearly 50°C and proceed to calculations with this value.

Table 3.9. Thermophysical properties of water at 50°C<sup>5</sup>

<b>Pr<sub>w</sub></b>	<b>Prandtl number of water</b>	3.59	
<b>k<sub>w</sub></b>	<b>Thermal conductivity of water</b>	642×10 <sup>-3</sup>	W/m•K
<b>ρ<sub>w</sub></b>	<b>Density of water</b>	988.142	kg/m <sup>3</sup>
<b>μ<sub>w</sub></b>	<b>Viscosity of water</b>	553×10 <sup>-6</sup>	N•s/m <sup>2</sup>

The Reynolds number, Nusselt number and the heat transfer coefficient of the water are calculated by the following formulas in the light of the information in the tables.

For Hydraulic Diameter on Water Side;

$$Dh_w = \frac{4 \times A_p}{S_p} = 0.02015 \quad (3.12)$$

For Reynolds Number on Water Side;

$$Re_w = \frac{\rho_w \times v_w \times Dh_w}{\mu_w} = 33872.75 \quad (3.13)$$

For Nusselt Number on Water Side;

$$Nu_w = 0.023 \times Re^{0.8} \times Pr^{0.4} = 161.3 \quad (3.14)$$

For Heat Transfer Coefficient on Water Side;

$$h_w = \frac{Nu_w \times k_w}{Dh_w} = 5139.32 \text{ W/m}^2\text{•K} \quad (3.15)$$

After these calculations, the heat transfer resistance is calculated. After calculated the heat transfer resistance, the combustion gas temperature is found by using the mapping temperatures. Later on, regional water temperatures are calculated. Regional

pipe outer surface temperatures are calculated by using the regional water temperature and heat transfer resistance.

After finding the pipe surface temperature at critical points by using heat transfer equations, it is checked that if this pipe surface temperature passes the dew point temperature values or not. The pipe outer surface temperatures are compared with the dew point temperature in table 2.3 depending % CO<sub>2</sub> ratio. This helps us to understand whether condensation occurs.

Table 3.10. Heat Transfer Resistance Calculation Parameters for the B type Cu HEx at min load (47/53°C)

$h_{fg}$	18.28	W/m <sup>2</sup> •K
$h_w$	5139.32	W/m <sup>2</sup> •K
$R_f''$	0.0002	m <sup>2</sup> •K/W
$A_{pi}$	0.0848	m <sup>2</sup>
$A_{po}$	0.0879	m <sup>2</sup>
$A_f$	1.0225	m <sup>2</sup>
$\eta_f$	0.832	
$N$	88	
$\eta_o$	0.854	
$\frac{1}{U \times A} = \sum R$	0.827	K/W

$\sum R$ ,  $\eta_f$  and  $\eta_o$  were calculated using the thermal resistance, fin efficiency, and overall surface efficiency formulas in the "*Fundamentals of heat and mass transfer*".<sup>5</sup> In addition that  $R_f''$  was taken from "*Representative Fouling Factors*" table.<sup>5</sup>

It was found the  $q = 8.91$  kW in Eq. 3.4. For mapping measurements, the exchanger area was split into 48 regions and used one risky region's CO<sub>2</sub> ratio. Because of this,  $q$  needs to distribute to 48 equal-area too.

Table 3.11. Gas Temperature Results for the B type Cu HEx at min load (47/53°C)

$q$	8910	W
$q_{1/48}$	185.625	W
$1/UA$	0.827	K/W
$T_{fg}$	66.90	°C
$T_{cg}$	220.52	°C

After calculating the heat which effects on the risky area, the regional water temperatures are calculated by using the following equation (3.16) to calculate the pipe outer surface temperature.

$$q = \dot{m} \times C_p \times \Delta T \quad (3.16)$$

With this formula, the temperature increase of the inlet water is approximately calculated.

Table 3.12. Mean Water Temperature Change Calculations for the B type Cu HEx at min load (47/53°C)

<b>q<sub>1/48</sub></b>	185.625	W		
<b><math>\dot{m}_w</math></b>	18	l/m	0.3	kg/s
<b>C<sub>p</sub><sub>w</sub></b>	4181	J/kg•K		
<b><math>\Delta T_w = \Delta T_{1/48}</math></b>	0.148	°C		

For risky region,  $\Delta T_w$  is found as 0.148°C. For every region of distributed 48 equal-area of the heat exchanger,  $\Delta T_{1/48}$  can be taken as 0.148°C.

The combustion gas, which is measured its CO<sub>2</sub> ratio and flue gas temperature over the HEx, passes through the 6<sup>th</sup> and 11<sup>th</sup> points of the divided heat exchanger when the water inlet side is taken as the zero points. And it is defined as the risky area for 47/53°C water cycle at min load.

The regional water temperatures are calculated by using following equation (3.17) in the light of the calculations at table 3.13.

$$T_{\text{regional water}} = T_{\text{water inlet}} + \text{Region Number} \times \Delta T_{1/48} \quad (3.17)$$

Table 3.13. Regional Water Temperatures at Risky Area for the B type Cu HEx at min load (47/53°C)

<b>T<sub>water inlet</sub></b>	47	°C
<b>T<sub>regional water 6<sup>th</sup></sub></b>	47.88	°C
<b>T<sub>regional water 11<sup>th</sup></sub></b>	48.62	°C

As the last step of to find the pipe outer surface temperatures, equation 3.18 is used for calculations.

$$T_{\text{regional pipe outer surface}} = q_{\text{net1/48}} \times \sum R_{\text{water to pos}} + T_{\text{regional water}} \quad (3.18)$$

Table 3.14. Regional Pipe Outer Surface Temperatures at Risky Area for the B type Cu HEx at min load (47/53°C)

$q_{1/48}$	185.625	W
$\sum R_{\text{water to pos}}$	0.00464	°C /W
$T_{\text{regional pipe outer surface 6}^{\text{th}}}$	48.75	°C
$T_{\text{regional pipe outer surface 11}^{\text{th}}}$	49.49	°C

The dew point value indicated in Table 2.3 for %3.00 CO<sub>2</sub> ratio is specified as 33.8°C. Since the pipe outer surface temperature through those areas of the heat exchanger is 48.56°C and does not go below 33.8°C, no condensation is observed in this region and in these operating conditions of the appliance. This was also physically controlled.

In the following tables and graphs, the percent of the carbon dioxide rate and flue gas temperature distribution are given for the **copper** heat exchanger of the **C type conventional appliance**.

Table 3.15. %CO<sub>2</sub> rate distribution over the C type Cu HEx at min load (47/53°C)

MIN 47/53°C								
Back side of heat exchanger								
CO2 (%)								
1,61	1,99	1,81	1,72	2,01	1,75	1,67	1,59	
2,41	1,82	2,47	2,32	2,57	2,11	1,99	1,93	
2,90	2,74	2,67	2,88	2,93	2,63	2,65	2,51	
2,61	1,99	3,15	2,82	3,12	2,42	2,57	2,77	
2,01	2,11	2,78	2,65	3,30	2,42	2,04	1,99	
1,78	2,32	2,11	1,83	1,94	2,23	1,87	1,71	
front side of heat exchanger								

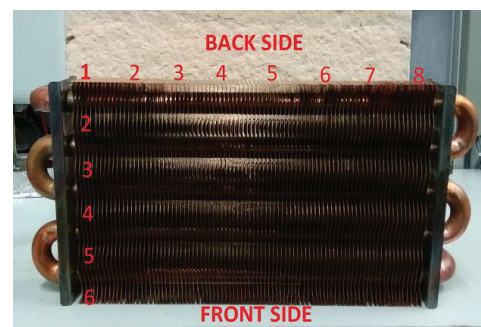


Figure 3.5. Mapping points on the Cu HEx



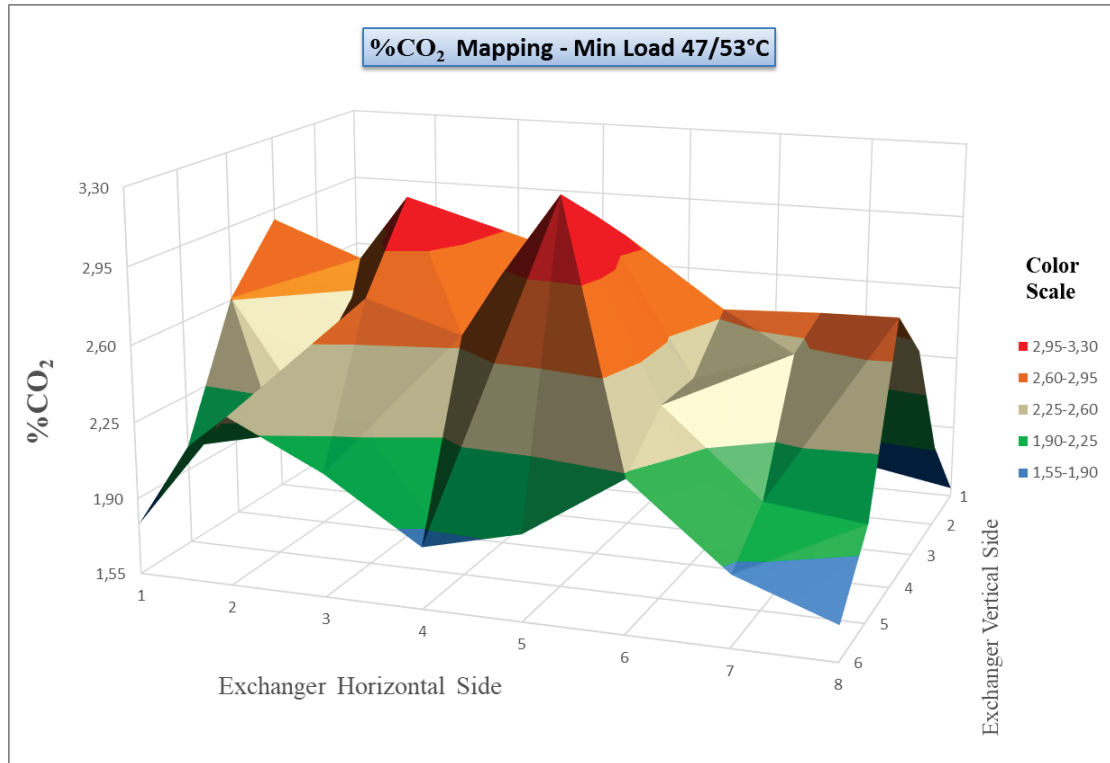
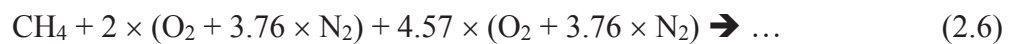


Figure 3.9. %CO<sub>2</sub> rate distribution over the Cu HEx at min load (47/53°C) for C type appliance

The critical point was defined as the EVS5 X EHS5 point over the heat exchanger, where both **low temperature (70.1°C)** and the **high CO<sub>2</sub> (%3.30)** rate. According to the calculations made using **CO<sub>2</sub> ratio 3.30%** and using equation 2.6, the excess air amount  $\lambda = 4.57$ , the **N<sub>2</sub>** and **O<sub>2</sub>** ratios in the flue gas in this region is **81.59%** and **15.10%** respectively. These values serve us to calculate the Prandtl, viscosity, density and thermal conductivity to be used for the heat transfer of airside. The sum of **CO<sub>2</sub>**, **N<sub>2</sub>** and **O<sub>2</sub>** ratios is **99.99%**.

Once we had calculated excess air quantity ( $\lambda$ ), we had also been able to calculate how much air will be required for 1 m<sup>3</sup> CH<sub>4</sub>.



$$\text{For } 1 \text{ m}^3 \text{ CH}_4 \rightarrow 6.57 \text{ m}^3 \text{ O}_2 + 24.72 \text{ m}^3 \text{ N}_2 = 31.30 \text{ m}^3 \text{ air is required.} \quad (3.19)$$

Heat output and efficiency are the same value with B type appliance. Since the gas used in the tests does not change, the gas net calorimetric value is also the same. Therefore the amount of gas used does not change.

The used gas flow rate:  $\dot{V}_g = 0.94 \text{ m}^3/\text{h}$  (3.5)

For  $0.94 \text{ m}^3/\text{h}$  test gas  $\rightarrow$   $29.52 \text{ m}^3/\text{h}$  fresh air is used during the test which performed under the stated operating conditions.

At the tests which had the same operating conditions and using the same exchanger but in two different appliances as B type and C type combi boiler, the combustion gases were measured at different ratios and at different temperatures as we had seen in  $47/53^\circ\text{C}$  mapping tests. The reason for that is the amount of fresh air used in the two products is different.

Table 3.16. Temperature distribution over the C type Cu HEx at min load ( $47/53^\circ\text{C}$ )

MIN 47/53°C							
Back side of heat exchanger							
Temperature (°C)							
71,1	73,2	74,4	77,7	76,3	77,8	71,9	74,3
70,1	75,3	67,4	69,9	76,1	73,3	64,6	66,6
68,8	68,1	71,1	75,6	73,9	74,1	69,8	70,3
65,1	66,1	70,8	72,3	75,1	68,9	62,3	66,1
59,8	58,2	62,3	65,4	70,1	65,1	66,8	65,7
58,9	59,2	63,1	60,3	64,2	63,4	60,1	59,7
front side of heat exchanger							

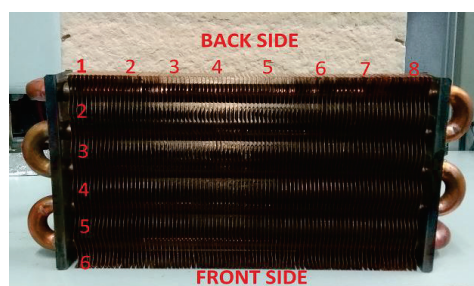


Figure 3.5. Mapping points on the Cu HEx

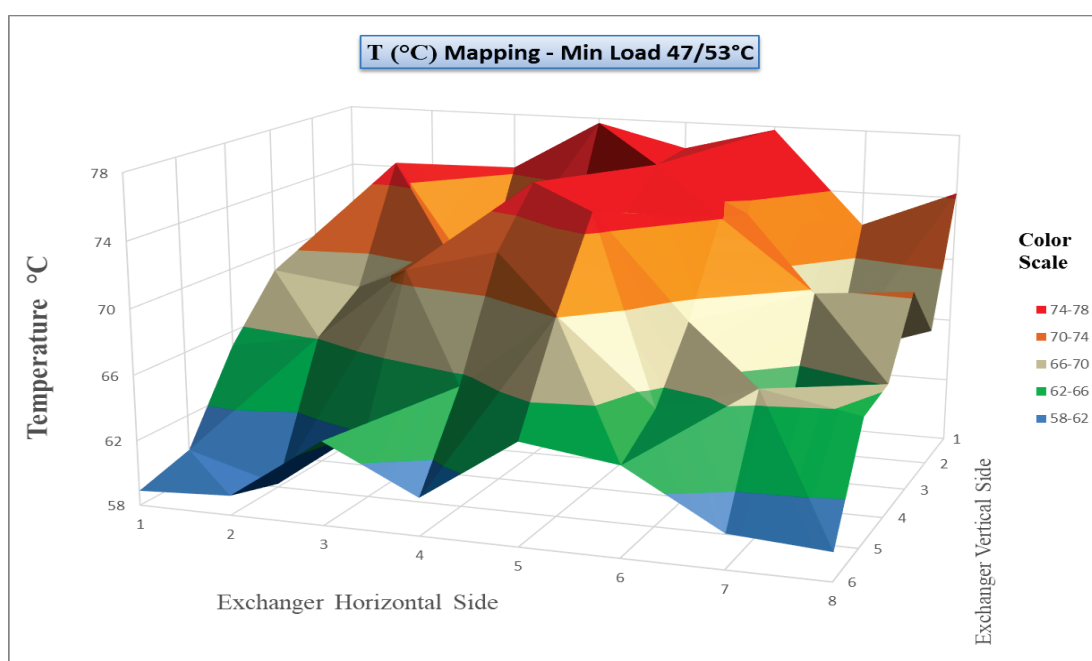


Figure 3.10. Temperature distribution over the Cu HEx at min load ( $47/53^\circ\text{C}$ ) for C type appliance

Density, viscosity, Prandtl number and thermal conductivity values of CO<sub>2</sub>, N<sub>2</sub>, and O<sub>2</sub> for 147°C were taken from the thermophysical properties table<sup>5</sup> in order to calculate those values of the flue gas side.

Table 3.17. Thermophysical properties of Flue gas for the C type Cu HEx at min load (47/53°C)

<b>Flue gas content (N<sub>2</sub> + CO<sub>2</sub> + O<sub>2</sub>) = 0.99</b>	0.816	0.033	0.151
<b>Pr<sub>fg</sub> Prandtl number of flue gas</b>	0.7101		
<b>k<sub>fg</sub> Thermal conductivity of flue gas</b>	33.6×10 <sup>-3</sup>	W/m•K	
<b>ρ<sub>fg</sub> Density of flue gas</b>	0.846	kg/m <sup>3</sup>	
<b>μ<sub>fg</sub> Viscosity of flue gas</b>	2.33×10 <sup>-5</sup>	N•s/m <sup>2</sup>	

As the amount of fresh air changes, the gas flow rate also changes. A<sub>fg</sub> and Dh<sub>Cu</sub> remain the same values because the same heat exchanger with B type appliance is used. Depending on the gas flow rate, the gas velocity changes and the Re<sub>fg</sub>, Nu<sub>fg</sub> and h<sub>fg</sub> values for the B type appliance are given in the table 3.18. Since the exchanger parameters and the amount of inlet water do not change, the water side Re<sub>w</sub>, Nu<sub>w</sub> and h<sub>w</sub> remain the same as in the B type device. All calculations are given in table 3.18.

Table 3.18. Results for Re and Nu numbers and h value of both Flue Gas and Water Side for the C type Cu HEx at min load (47/53°C)

<b>Gas flow rate (G20)</b>	30.46	m <sup>3</sup> /h
<b>v<sub>g</sub> Gas velocity</b>	0.46	m/s
<b>Re<sub>fg</sub></b>	31.40	
<b>Nu<sub>fg</sub></b>	0.95	
<b>h<sub>fg</sub></b>	17.23	W/m <sup>2</sup> •K
<b>Re<sub>w</sub></b>	33872.75	
<b>Nu<sub>w</sub></b>	161.30	
<b>h<sub>w</sub></b>	5139.32	W/m <sup>2</sup> •K

Since it is the same with B type appliance as the exchanger parameters and the h<sub>w</sub>, only the values influenced by h<sub>fg</sub> exchange are shared in table 3.19.

Table 3.19. Heat Transfer Resistance and Gas Temperatures Results for the C type Cu HEx at min load (47/53°C)

$\eta_f$	0.840	
$\eta_o$	0.852	
$h_{fg}$	17.23	W/m <sup>2</sup> •K
$1/UA$	0.877	K/W
$q$	8.91	kW
$q_{1/48}$	185.625	W
$T_{fg}$	70.1	°C
$T_{cg}$	232.9	°C

The combustion gas, which is measured its CO<sub>2</sub> ratio and flue gas temperature over the HEx, passes through the 4<sup>th</sup> and 13<sup>th</sup> points of the divided heat exchanger when the water inlet side is taken as the zero points. And it is defined as the risky area for 47/53°C water cycle at min load for C type appliance.

Table 3.20. Regional Water and Pipe Outer Surface Temperatures at Risky Area for the C type Cu HEx at min load (47/53°C)

$T_{\text{water inlet}}$	47	°C
$T_{\text{regional water 4}^{\text{th}}}$	47.59	°C
$T_{\text{regional water 13}^{\text{th}}}$	48.92	°C
$q_{1/48}$	185.625	W
$\sum R_{\text{water to pos}}$	0.00466	°C /W
$T_{\text{regional pipe outer surface 4}^{\text{th}}}$	48.45	°C
$T_{\text{regional pipe outer surface 13}^{\text{th}}}$	49.78	°C

The dew point value indicated in Table 2.3 for %3.30 CO<sub>2</sub> ratio is specified as 34.6°C. Since the pipe outer surface temperature through those areas of the heat exchanger is 48.40°C and does not go below 34.6°C, no condensation is observed in this region and in these operating conditions of the appliance. This was also physically controlled.

The minimum load conditions and 47/53°C operating conditions for both temperature distributions and CO<sub>2</sub> ratios are far from the dew points. For this reason, these values which are similar for the stainless steel exchanger were not given as a graph.

At this point, the results of 60/80°C values and maximum load conditions observed as the critical dew conditions.

### 3.2.2. Mapping Results at Max Load & Calculations

As the second stage of the condensation tests, the tests were carried out under the max load condition. The reason for choosing 60/80°C in the shared data of these tests made according to the standards is having high CO<sub>2</sub> ratios. Even though there is no condensation risk for 60/80°C water cycle because of the high pipe outer surface temperatures, there is still condensation risk for transition cycles which start from the low inlet-outlet temperatures to 60/80°C. Here it was calculated which inlet and outlet temperatures the condensation will start.

In the following tables and graphs, the percent of the carbon dioxide rate and flue gas temperature distribution are given for the **copper** heat exchanger of the **B type conventional appliance**.

Table 3.21. %CO<sub>2</sub> rate distribution over the B type Cu HEx at max load (60/80°C)

MAX 60/80°C							
Back side of heat exchanger							
CO <sub>2</sub> (%)							
5,72	5,61	5,32	5,17	4,91	4,82	4,10	4,65
8,22	8,47	8,61	8,79	8,42	8,37	7,90	8,11
7,77	8,01	8,32	8,47	8,25	7,81	7,68	7,82
8,32	7,62	8,25	8,87	8,32	8,06	7,65	8,01
7,45	7,68	7,95	8,17	8,06	7,89	7,52	7,65
5,65	5,98	5,78	4,65	5,95	4,98	5,36	5,80
front side of heat exchanger							

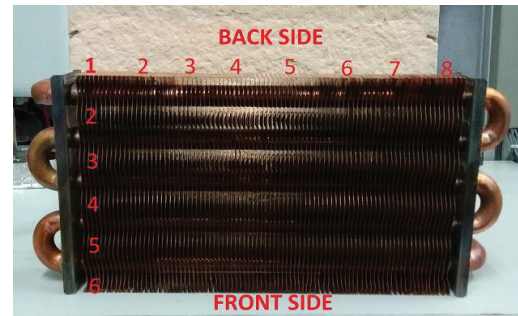


Figure 3.3. Mapping points on the Cu HEx

The critical point was defined as the EVS4 X EHS4 point over the heat exchanger, where both **low temperature (120°C)** and the **high CO<sub>2</sub> (%8.87)** rate. According to the calculations made using CO<sub>2</sub> ratio **8.87%** and using equation 2.6, the excess air amount  $\lambda = 0.58$ , the N<sub>2</sub> and O<sub>2</sub> ratios in the flue gas in this region is **85.99%** and **5.13%** respectively. These values serve us to calculate the Prandtl, viscosity, density and thermal conductivity to be used for the heat transfer of airside. The sum of CO<sub>2</sub>, N<sub>2</sub> and O<sub>2</sub> ratios is **99.99%**.

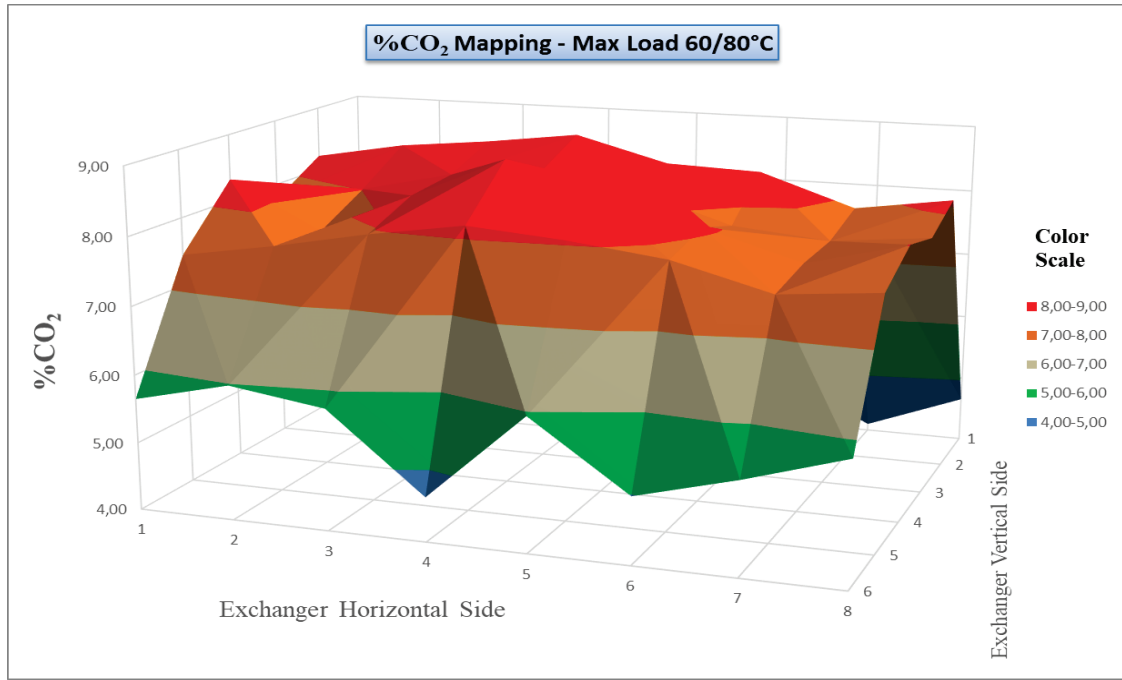
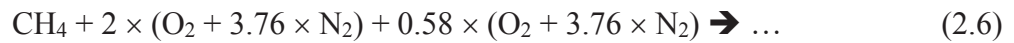


Figure 3.11. %CO<sub>2</sub> rate distribution over the Cu HEx at max load (60/80°C) for B type appliance

Once we had calculated excess air quantity ( $\lambda$ ), we had also been able to calculate how much air will be required for 1 m<sup>3</sup> CH<sub>4</sub>.



$$\text{For 1 m}^3 \text{ CH}_4 \rightarrow 2.58 \text{ m}^3 \text{ O}_2 + 9.69 \text{ m}^3 \text{ N}_2 = 12.27 \text{ m}^3 \text{ air is required.} \quad (3.20)$$

For max load measurement:  $Q_o = 24 \text{ kW}$

In equations 3.21,  $Q_i$  was found according to the calculation which was made in Equation 3.3.

$$\text{So; } Q_i = 26.73 \text{ kW} \quad (3.21)$$

For gas flow rate; ( $H_i = 34.02 \text{ MJ/m}^3$  for G20)

$$\dot{V}_g = \frac{Q_i}{H_i} = 2.82 \text{ m}^3/\text{h} \quad (3.22)$$

The heat input ( $Q_i$ ) is calculated by the program in the test rig using the eq. 3.6. From the test rig data it is seen that the gas amount ( $\dot{V}_g$ ) is 2.80 m<sup>3</sup>/h and the heat input ( $Q_i$ ) from its calculations is 26.7 kW.

As can be seen from the differences between the calculations, there is a deviation of 0.8% in gas flow rate ( $\dot{V}_g$ ) and 0.2% in heat input ( $Q_i$ ). These deviations, which are not more than 1%, can be ignored and calculations methods in equation 3.21 and 3.22 can be used instead of test rig data from the performed test.

In equation 3.20 we found that 12.27 m<sup>3</sup> of fresh air is needed for 1 m<sup>3</sup> of CH<sub>4</sub> gas. In equation 3.22, we calculated that the appliance consumes a total of 2.82 m<sup>3</sup>/h gas during the tests. From here;

For 2.82 m<sup>3</sup>/h test gas → 34.72 m<sup>3</sup>/h fresh air is used during the test which performed under the stated operating conditions.

Table 3.22. Temperature distribution over the B type Cu HEx at max load (60/80°C)

MAX 60/80°C							
Back side of heat exchanger							
Temperature (°C)							
117,9	129,8	135,6	132,5	126,7	142,1	133,6	128,4
130,9	131,2	137,6	128,8	129,7	134,1	129,2	132,6
125,9	135,9	133,4	128,8	129,2	124,6	125,5	126,4
113,3	131,1	127,7	120,0	122,1	118,7	111,6	121,3
111,9	109,8	115,4	117,2	108,8	112,9	101,1	107,6
115,7	119,8	107,8	124,4	121,9	112,8	107,7	113,8
front side of heat exchanger							

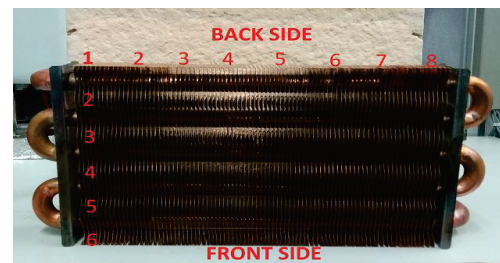


Figure 3.3. Mapping points on the Cu HEx

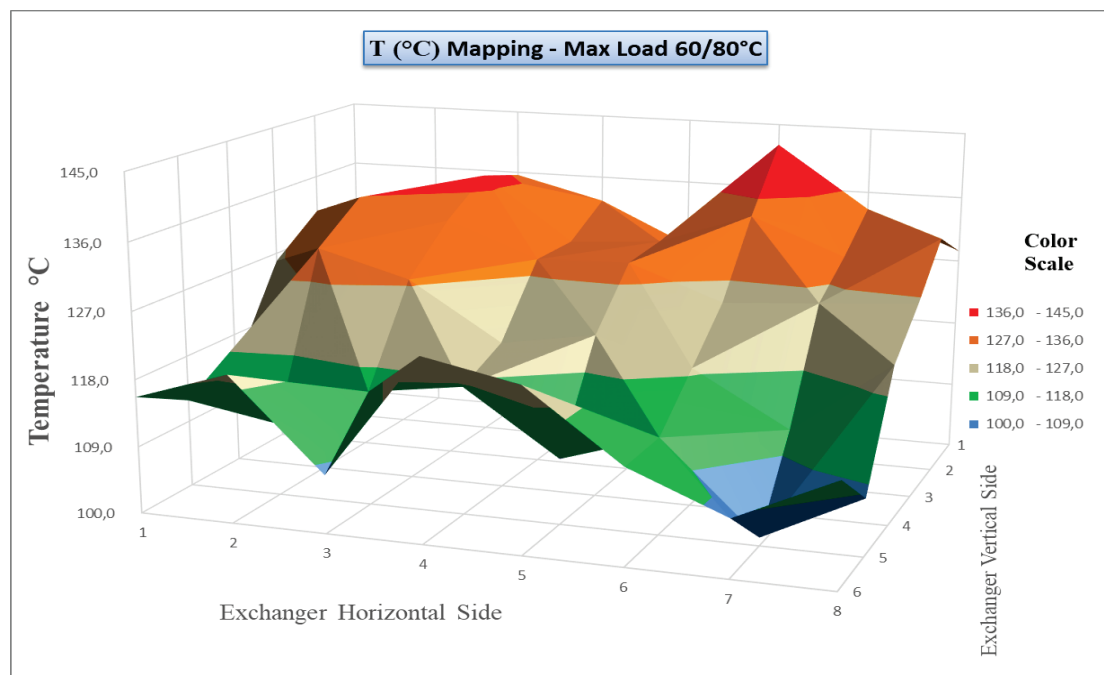


Figure 3.12. Temperature distribution over the Cu HEx at max load (60/80°C) for B type appliance

Density, viscosity, Prandtl number and thermal conductivity values of CO<sub>2</sub>, N<sub>2</sub>, and O<sub>2</sub> for 357°C were taken from the thermophysical properties table<sup>5</sup> in order to calculate those values of the flue gas side.

Table 3.23. Thermophysical properties of CO<sub>2</sub>, N<sub>2</sub> and O<sub>2</sub> at 357°C<sup>5</sup>

<b>T<sub>fga</sub></b>	<b>Average flue gas temperature</b>	357	°C
<b>Pr<sub>N2</sub></b>	<b>Prandtl number of N<sub>2</sub></b>	0.703	
<b>Pr<sub>CO2</sub></b>	<b>Prandtl number of CO<sub>2</sub></b>	0.714	
<b>Pr<sub>O2</sub></b>	<b>Prandtl number of O<sub>2</sub></b>	0.734	
<b>k<sub>N2</sub></b>	<b>Thermal conductivity of N<sub>2</sub></b>	46.3×10 <sup>-3</sup>	W/m•K
<b>k<sub>CO2</sub></b>	<b>Thermal conductivity of CO<sub>2</sub></b>	43.1×10 <sup>-3</sup>	W/m•K
<b>k<sub>O2</sub></b>	<b>Thermal conductivity of O<sub>2</sub></b>	48.9×10 <sup>-3</sup>	W/m•K
<b>ρ<sub>N2</sub></b>	<b>Density of N<sub>2</sub></b>	0.534	kg/m <sup>3</sup>
<b>ρ<sub>CO2</sub></b>	<b>Density of CO<sub>2</sub></b>	0.838	kg/m <sup>3</sup>
<b>ρ<sub>O2</sub></b>	<b>Density of O<sub>2</sub></b>	0.609	kg/m <sup>3</sup>
<b>μ<sub>N2</sub></b>	<b>Viscosity of N<sub>2</sub></b>	3.01×10 <sup>-5</sup>	N•s/m <sup>2</sup>
<b>μ<sub>CO2</sub></b>	<b>Viscosity of CO<sub>2</sub></b>	2.81×10 <sup>-5</sup>	N•s/m <sup>2</sup>
<b>μ<sub>O2</sub></b>	<b>Viscosity of O<sub>2</sub></b>	3.56×10 <sup>-5</sup>	N•s/m <sup>2</sup>

After these values were found, density, viscosity, Prandtl number and thermal conductivity values of the flue gas side are calculated by multiplying the ratios of CO<sub>2</sub>, N<sub>2</sub>, and O<sub>2</sub> in the flue gas. The values in Table 3.23 were multiplied by the CO<sub>2</sub>, N<sub>2</sub> and O<sub>2</sub> ratios in the flue gas and thus the flue gas values in Table 3.24 were calculated.

Table 3.24. Thermophysical properties of Flue gas the B type Cu HEx at max load (60/80°C)

<b>Flue gas content (N<sub>2</sub> + CO<sub>2</sub> + O<sub>2</sub>) = 0.99</b>	0.86	0.0887	0.051
<b>Pr<sub>fg</sub></b>	<b>Prandtl number of flue gas</b>	0.7055	
<b>k<sub>fg</sub></b>	<b>Thermal conductivity of flue gas</b>	46.1×10 <sup>-3</sup>	W/m•K
<b>ρ<sub>fg</sub></b>	<b>Density of flue gas</b>	0.461	kg/m <sup>3</sup>
<b>μ<sub>fg</sub></b>	<b>Viscosity of flue gas</b>	3.02×10 <sup>-5</sup>	N•s/m <sup>2</sup>



Table 3.25 shows some the thermophysical properties such as density, viscosity, Prandtl number and thermal conductivity values at 70°C, which is the average temperature for water 60/80°C tests.

Table 3.25. Thermophysical properties of water at 70°C<sup>5</sup>

<b>Pr<sub>w</sub></b>	<b>Prandtl number of water</b>	2.52	
<b>k<sub>w</sub></b>	<b>Thermal conductivity of water</b>	677×10 <sup>-3</sup>	W/m•K
<b>ρ<sub>w</sub></b>	<b>Density of water</b>	977.622	kg/m <sup>3</sup>
<b>μ<sub>w</sub></b>	<b>Viscosity of water</b>	400×10 <sup>-6</sup>	N•s/m <sup>2</sup>

Since the copper exchanger used in tests 47/53°C is also used in tests 60/80°C, the exchanger parameters are the same as those used in previous calculations. As the amount of gas consumed and the amount of required fresh air changed, the gas flow rate and gas velocity changed. In addition, the water side heat transfer coefficient has also changed because of the average water temperature changed in 60/80°C tests compared with 47/53°C tests.

Table 3.26. Results for Re and Nu numbers and h value of both Flue Gas and Water Side for the B type Cu HEx at max load (60/80°C)

<b>Gas flow rate (G20)</b>	37.55	m <sup>3</sup> /h
<b>v<sub>g</sub> Gas velocity</b>	0.57	m/s
<b>Re<sub>fg</sub></b>	19.86	
<b>Nu<sub>fg</sub></b>	0.70	
<b>h<sub>fg</sub></b>	17.37	W/m <sup>2</sup> •K
<b>Re<sub>w</sub></b>	46276.16	
<b>Nu<sub>w</sub></b>	179.76	
<b>h<sub>w</sub></b>	6043.57	W/m <sup>2</sup> •K

Since it is the same exchanger parameters with 47/53°C tests appliance, the values influenced by h<sub>fg</sub> and h<sub>w</sub> exchange are shared in table 3.27.

Table 3.27. Heat Transfer Resistance and Gas Temperatures Results for the B type Cu HEx at max load (60/80°C)

$\eta_f$	0.839	
$\eta_o$	0.851	
$h_{fg}$	17.37	W/m <sup>2</sup> •K
$1/UA$	0.869	K/W
$q$	26.73	kW
$q_{1/48}$	556.875	W
$T_{fg}$	120	°C
$T_{cg}$	604.31	°C

The combustion gas, which is measured its CO<sub>2</sub> ratio and flue gas temperature over the HEx, passes through the 12<sup>th</sup> and 21<sup>st</sup> points of the divided heat exchanger when the water inlet side is taken as the zero points. And it is defined as the risky area for 60/80°C water cycle at max load for B type appliance.

Table 3.28. Regional Water and Pipe Outer Surface Temperatures at Risky Area for the B type Cu HEx at max load (60/80°C)

$C_{pw}$	4190	J/kg•K
$\Delta T_w = \Delta T_{1/48}$	0.443	°C
$T_{\text{water inlet}}$	60	°C
$T_{\text{regional water 12}^{\text{th}}}$	65.31	°C
$T_{\text{regional water 21}^{\text{st}}}$	69.30	°C
$q_{\text{net1/48}}$	556.875	W
$\sum R_{\text{water to pos}}$	0.00432	°C /W
$T_{\text{regional pipe outer surface 12}^{\text{th}}}$	67.72	°C
$T_{\text{regional pipe outer surface 21}^{\text{st}}}$	71.70	°C

The dew point value indicated in Table 2.3 for %8.87 CO<sub>2</sub> ratio is specified as 52.8°C. Since the pipe outer surface temperatures through those areas of the heat exchanger are 67.71°C and 71.70°C, and does not go below 52.8°C, no condensation is observed in this region and in these operating conditions of the appliance. This was also physically controlled.

As it is mentioned in the entry of the max load mapping results section, condensation occurrence is not observed for 60/80°C inlet-outlet water cycle. The high pipe outer surface temperatures occurred with the influence of the high water temperature in the circulation do not allow the condensation occurrence. But there is a still condensation occurrence risk until the water temperature in circulation reaches to the 60/80°C inlet-outlet water cycle. By way of changing the inlet water temperature in these calculations, the critical temperatures for condensation occurrence can be found.

According to calculations, condensation occurrence can be observed until inlet water temperatures reach up to 46°C. When the water enters the cycle at 46°C, the temperatures of the pipe outer surfaces which contact with combustion gas are 53.7°C and 57.7°C. Since the dew point value indicated in Table 2.3 for %8.87 CO<sub>2</sub> ratio is specified as 52.8°C, condensation stops after 46°C water inlet temperature.

In the following tables and graphs, the percent of the carbon dioxide rate and flue gas temperature distribution are given for the **copper** heat exchanger of the **C type conventional appliance**.

Table 3.29. %CO<sub>2</sub> rate distribution over the C type Cu HEx at max load (60/80°C)

MAX 60/80°C								
Back side of heat exchanger								
CO <sub>2</sub> (%)								
4,27	4,18	3,52	3,31	5,15	2,72	3,54	4,22	
3,78	3,65	5,03	5,21	5,57	5,41	4,62	3,82	
5,41	5,29	5,11	5,37	5,65	5,48	5,06	5,15	
4,98	4,61	5,11	6,02	5,78	5,88	5,32	4,87	
4,17	4,61	5,03	6,03	6,47	6,10	4,72	4,68	
3,10	4,89	2,87	3,21	2,99	3,61	3,25	4,17	
front side of heat exchanger								

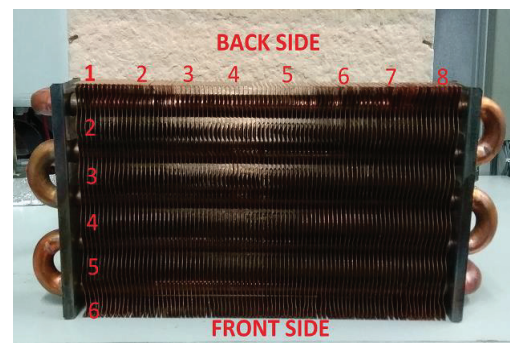


Figure 3.5. Mapping points on the Cu HEx

The critical point was defined as the EVS5 X EHS6 point over the heat exchanger, where both **low temperature (112°C)** and the **high CO<sub>2</sub> (%6.10)** rate. According to the calculations made using CO<sub>2</sub> ratio **6.10%** and using equation 2.6, the excess air amount  $\lambda = 1.65$ , the N<sub>2</sub> and O<sub>2</sub> ratios in the flue gas in this region is **83.81%** and **10.08%** respectively. These values serve us to calculate the Prandtl, viscosity, density and thermal conductivity to be used for the heat transfer of airside. The sum of CO<sub>2</sub>, N<sub>2</sub> and O<sub>2</sub> ratios is **99.99%**.

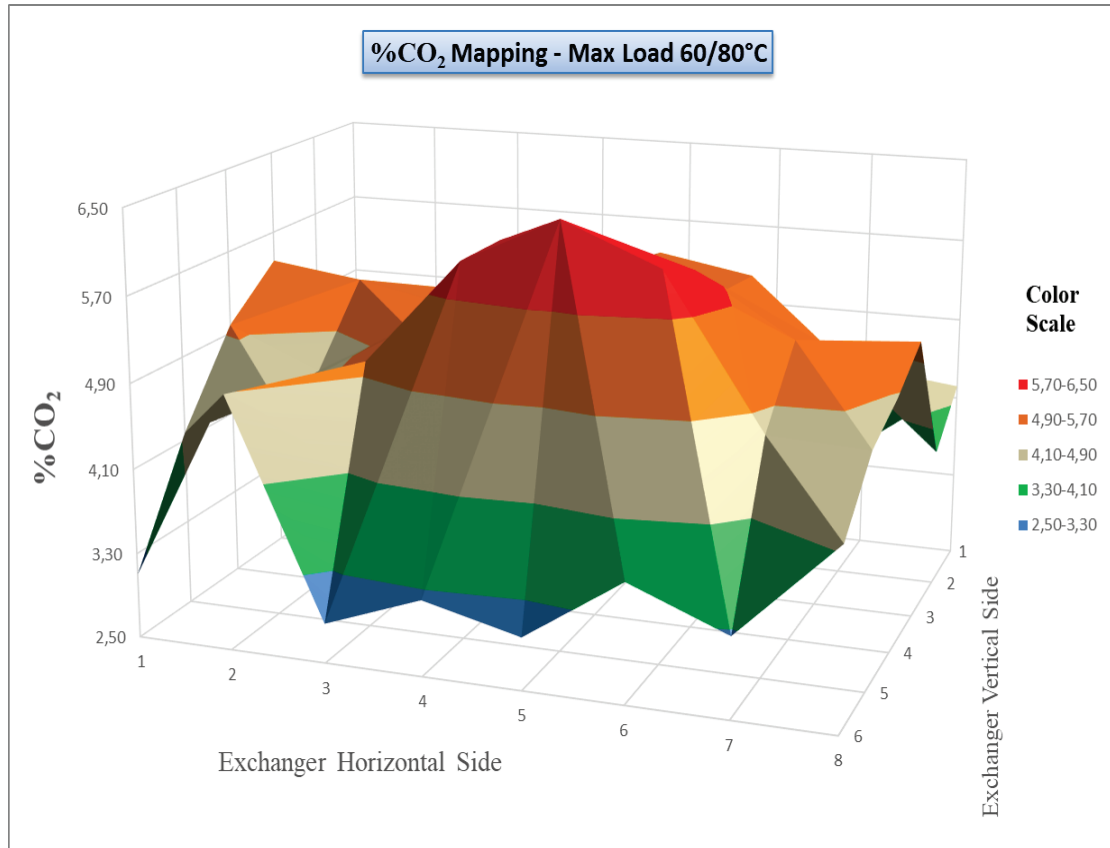
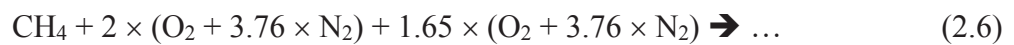


Figure 3.13. %CO<sub>2</sub> rate distribution over the Cu HEx at max load (60/80°C) for C type appliance

Once we had calculated excess air quantity ( $\lambda$ ), we had also been able to calculate how much air will be required for 1 m<sup>3</sup> CH<sub>4</sub>.



$$\text{For } 1 \text{ m}^3 \text{ CH}_4 \rightarrow 3.65 \text{ m}^3 \text{ O}_2 + 13.74 \text{ m}^3 \text{ N}_2 = 17.39 \text{ m}^3 \text{ air is required.} \quad (3.23)$$

Heat output and efficiency are the same value with B type appliance. Since the gas used in the tests does not change, the gas net calorimetric value is also the same. Therefore the amount of gas used does not change.

The used gas flow rate  $\dot{V}_g = 2.82 \text{ m}^3/\text{h}$

For 2.82 m<sup>3</sup>/h test gas  $\rightarrow$  49.21 m<sup>3</sup>/h fresh air is used during the test which performed under the stated operating conditions.

Table 3.30. Temperature distribution over the C type Cu HEx at max load (60/80°C)

MAX 60/80°C							
Back side of heat exchanger							
Temperature (°C)							
137,8	134,5	141,6	146,6	132,6	144,5	129,5	131,8
118,9	128,9	141,1	135,4	143,4	147,7	131,9	120,9
131,2	124,6	125,5	138,7	144,4	142,8	136,1	128,9
127,7	119,8	117,8	134,9	139,8	136,6	140,1	121,9
107,8	101,9	109,8	121,2	134,2	112	131,1	112,3
98,7	104,9	111,6	102,9	117,8	96,6	113,5	101,3
front side of heat exchanger							

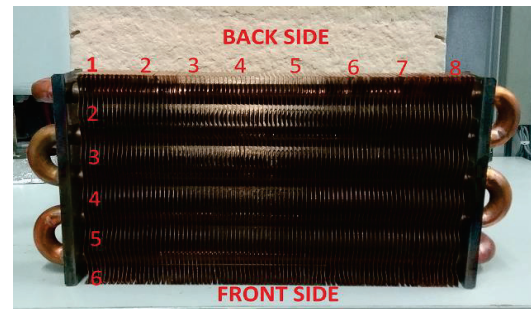


Figure 3.5. Mapping points on the Cu HEx

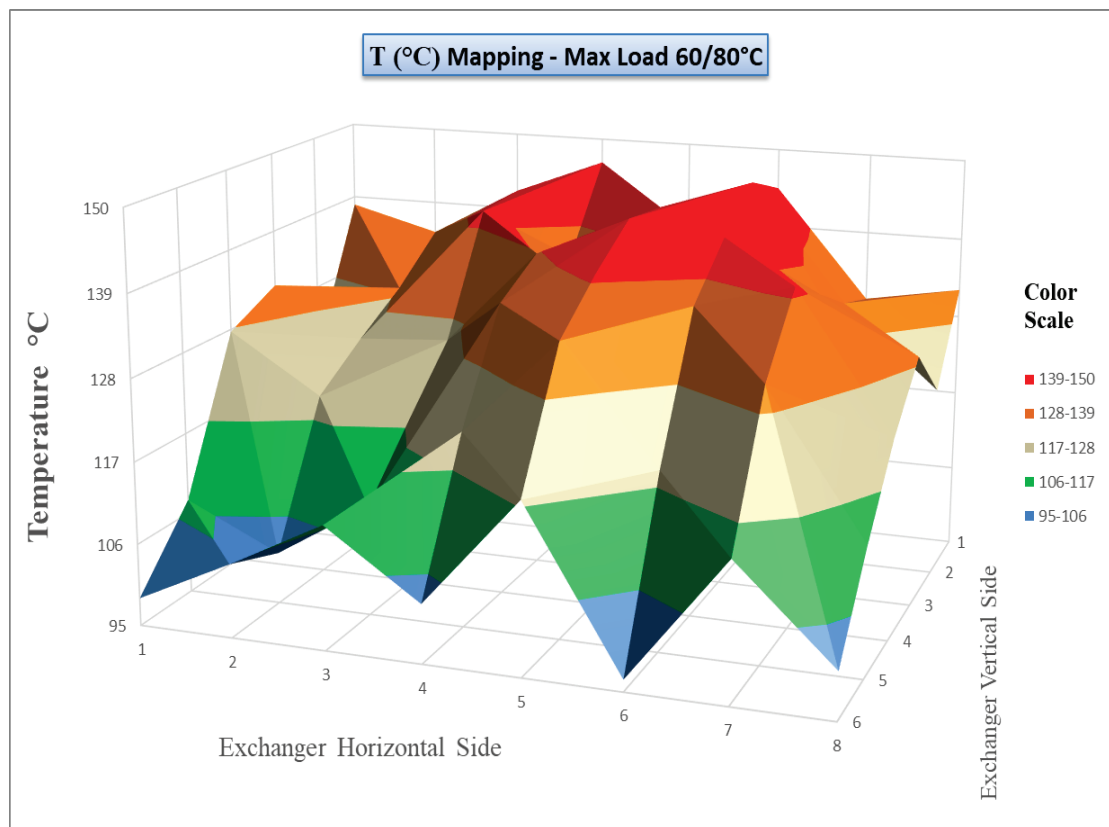


Figure 3.14. Temperature distribution over the Cu HEx at max load (60/80°C) for C type appliance

Density, viscosity, Prandtl number and thermal conductivity values of CO<sub>2</sub>, N<sub>2</sub>, and O<sub>2</sub> for 325°C were taken from the thermophysical properties table<sup>5</sup> in order to calculate those values of the flue gas side.

Table 3.31. Thermophysical properties of CO<sub>2</sub>, N<sub>2</sub> and O<sub>2</sub> at 325°C<sup>5</sup>

<b>T<sub>fga</sub></b>	<b>Average flue gas temperature</b>	325	°C
<b>Pr<sub>N2</sub></b>	<b>Prandtl number of N<sub>2</sub></b>	0.701	
<b>Pr<sub>CO2</sub></b>	<b>Prandtl number of CO<sub>2</sub></b>	0.717	
<b>Pr<sub>O2</sub></b>	<b>Prandtl number of O<sub>2</sub></b>	0.729	
<b>k<sub>N2</sub></b>	<b>Thermal conductivity of N<sub>2</sub></b>	44.6×10 <sup>-3</sup>	W/m•K
<b>k<sub>CO2</sub></b>	<b>Thermal conductivity of CO<sub>2</sub></b>	40.7×10 <sup>-3</sup>	W/m•K
<b>k<sub>O2</sub></b>	<b>Thermal conductivity of O<sub>2</sub></b>	47.3×10 <sup>-3</sup>	W/m•K
<b>ρ<sub>N2</sub></b>	<b>Density of N<sub>2</sub></b>	0.561	kg/m <sup>3</sup>
<b>ρ<sub>CO2</sub></b>	<b>Density of CO<sub>2</sub></b>	0.882	kg/m <sup>3</sup>
<b>ρ<sub>O2</sub></b>	<b>Density of O<sub>2</sub></b>	0.641	kg/m <sup>3</sup>
<b>μ<sub>N2</sub></b>	<b>Viscosity of N<sub>2</sub></b>	2.90×10 <sup>-5</sup>	N•s/m <sup>2</sup>
<b>μ<sub>CO2</sub></b>	<b>Viscosity of CO<sub>2</sub></b>	2.70×10 <sup>-5</sup>	N•s/m <sup>2</sup>
<b>μ<sub>O2</sub></b>	<b>Viscosity of O<sub>2</sub></b>	3.43×10 <sup>-5</sup>	N•s/m <sup>2</sup>

After these values were found, density, viscosity, Prandtl number and thermal conductivity values of the flue gas side are calculated by multiplying the ratios of CO<sub>2</sub>, N<sub>2</sub>, and O<sub>2</sub> in the flue gas. The values in Table 3.31 were multiplied by the CO<sub>2</sub>, N<sub>2</sub> and O<sub>2</sub> ratios in the flue gas and thus the flue gas values in Table 3.32 were calculated.

Table 3.32. Thermophysical properties of Flue gas for the C type Cu HEx at max load (60/80°C)

<b>Flue gas content (N<sub>2</sub> + CO<sub>2</sub> + O<sub>2</sub>) = 0.99</b>	0.838	0.061	0.10
<b>Pr<sub>fg</sub></b>	<b>Prandtl number of flue gas</b>	0.704	
<b>k<sub>fg</sub></b>	<b>Thermal conductivity of flue gas</b>	44.6×10 <sup>-3</sup>	W/m•K
<b>ρ<sub>fg</sub></b>	<b>Density of flue gas</b>	0.589	kg/m <sup>3</sup>
<b>μ<sub>fg</sub></b>	<b>Viscosity of flue gas</b>	2.94×10 <sup>-5</sup>	N•s/m <sup>2</sup>

As the amount of fresh air changes, the gas flow rate also changes. A<sub>fg</sub> and Dh<sub>Cu</sub> remain the same because the same heat exchanger with B type appliance is used. Depending on the gas flow rate, the gas velocity changes and the Re<sub>fg</sub>, Nu<sub>fg</sub> and h<sub>fg</sub> values

for the C type appliance are given in the table 3.33. Since the exchanger parameters and the amount of inlet water do not change, the water side  $Re_w$ ,  $Nu_w$  and  $h_w$  remain the same as in the B type appliance. All calculations are given in table 3.33.

Table 3.33. Results for Re and Nu numbers and h value of both Flue Gas and Water Side for the C type Cu HEx at max load (60/80°C)

<b>Gas flow rate (G20)</b>	52.04	m <sup>3</sup> /h
<b>v<sub>g</sub> Gas velocity</b>	0.79	m/s
<b>Re<sub>fg</sub></b>	29.47	
<b>Nu<sub>fg</sub></b>	0.91	
<b>h<sub>fg</sub></b>	21.85	W/m <sup>2</sup> •K
<b>Re<sub>w</sub></b>	46276.16	
<b>Nu<sub>w</sub></b>	179.76	
<b>h<sub>w</sub></b>	6043.57	W/m <sup>2</sup> •K

Since it is the same with B type appliance as the exchanger parameters and the  $h_w$ , only the values influenced by  $h_{fg}$  exchange are shared in table 3.34.

Table 3.34. Heat Transfer Resistance and Gas Temperatures Results for the C type Cu HEx at max load (60/80°C)

<b><math>\eta_f</math></b>	0.807	
<b><math>\eta_o</math></b>	0.822	
<b>h<sub>fg</sub></b>	21.85	W/m <sup>2</sup> •K
<b>1/UA</b>	0.752	K/W
<b>q</b>	26.73	kW
<b>q<sub>1/48</sub></b>	556.875	W
<b>T<sub>fg</sub></b>	112	°C
<b>T<sub>cg</sub></b>	531	°C

The combustion gas, which is measured its CO<sub>2</sub> ratio and flue gas temperature over the HEx, passes through the 3<sup>rd</sup> and 14<sup>th</sup> points of the divided heat exchanger when the water inlet side is taken as the zero points. And it is defined as the risky area for 60/80°C water cycle at max load for C type appliance.

Table 3.35. Regional Water and Pipe Outer Surface Temperatures at Risky Area for the C type Cu HEx at max load (60/80°C)

$T_{\text{water inlet}}$	60	°C
$T_{\text{regional water 3}^{\text{rd}}}$	61.32	°C
$T_{\text{regional water 14}^{\text{th}}}$	66.20	°C
$q_{\text{net1/48}}$	556.875	W
$\sum R_{\text{water to pos}}$	0.0043	°C /W
$T_{\text{regional pipe outer surface 3}^{\text{rd}}}$	63.73	°C
$T_{\text{regional pipe outer surface 14}^{\text{th}}}$	68.60	°C

The dew point value indicated in Table 2.3 for %6.10 CO<sub>2</sub> ratio is specified as 44.7°C. Since the pipe outer surface temperatures through those areas of the heat exchanger are 63.40°C and 68.60°C, and does not go below 44.7°C, no condensation is observed in this region and in these operating conditions of the appliance. This was also physically controlled.

According to calculations, condensation occurrence can be observed until inlet water temperatures reach up to 41°C. When the water enters the cycle at 41°C, the temperatures of the pipe outer surfaces which contact with combustion gas are 44.73°C and 49.6°C. Since the dew point value indicated in Table 2.3 for %6.10 CO<sub>2</sub> ratio is specified as 44.7°C, condensation stops after 41°C water inlet temperature.

In the following tables and graphs, the percent of the carbon dioxide rate and flue gas temperature distribution are given for the **stainless steel** heat exchanger of the **C type conventional appliance**.

Table 3.36. %CO<sub>2</sub> rate distribution over the C type SS HEx at max load (60/80°C)

MAX 60/80°C							
Back side of heat exchanger							
CO <sub>2</sub> (%)							
4,11	3,79	4,05	4,23	3,62	3,31	4,17	3,87
4,25	5,11	4,79	3,88	5,12	5,39	4,45	3,77
3,77	4,37	4,25	5,31	4,89	4,12	5,61	5,11
6,10	6,60	5,79	5,92	6,03	5,46	4,81	3,89
8,17	7,15	7,77	6,89	7,21	6,23	6,72	6,11
6,89	6,81	5,89	6,13	5,13	5,82	5,45	4,98
front side of heat exchanger							

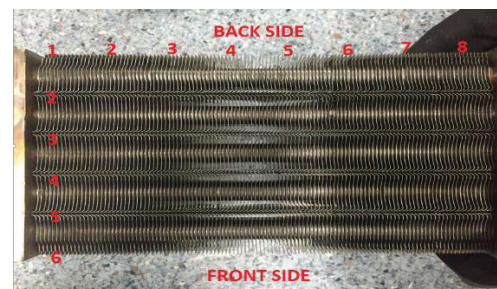


Figure 3.6. Mapping points on the SS HEx



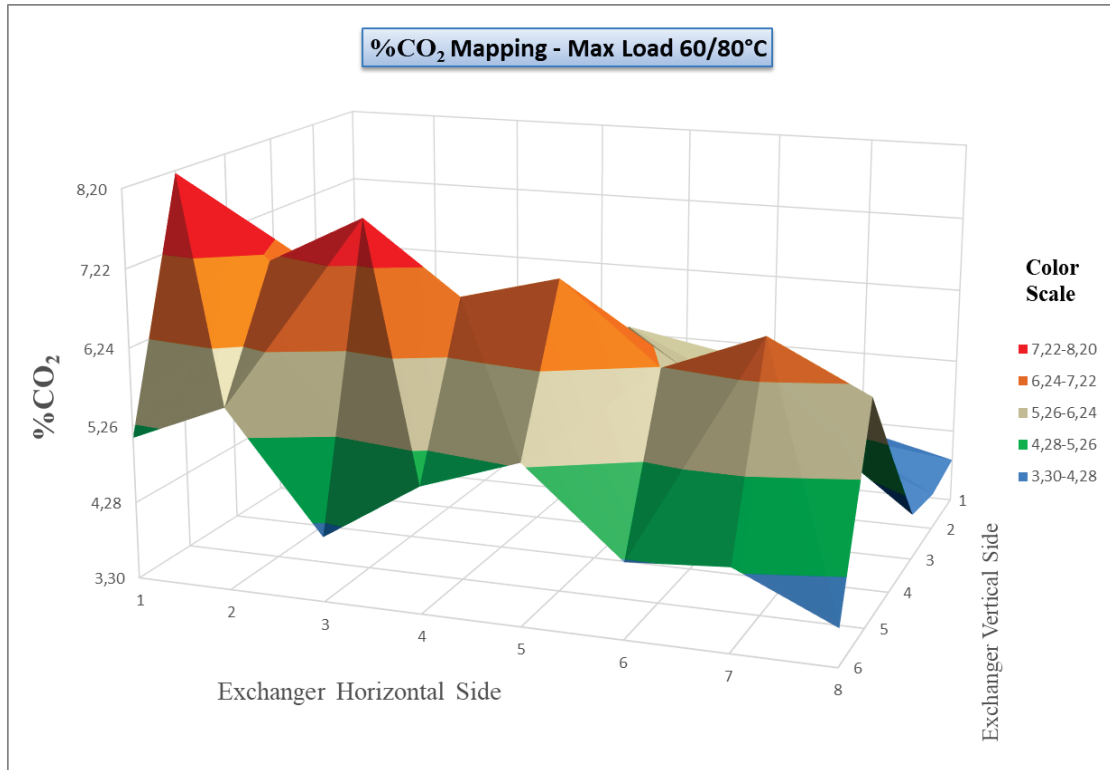
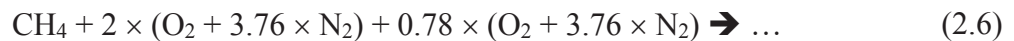


Figure 3.15. %CO<sub>2</sub> rate distribution over the SS HEx at max load (60/80°C) for C type appliance

The critical point was defined as the EVS5 X EHS1 point over the heat exchanger, where both **low temperature (115°C)** and the **high CO<sub>2</sub> (%8.17)** rate. According to the calculations made using CO<sub>2</sub> ratio **8.17%** and using equation 2.6, the excess air amount  $\lambda = 0.78$ , the N<sub>2</sub> and O<sub>2</sub> ratios in the flue gas in this region is **85.44%** and **6.38%** respectively. These values serve us to calculate the Prandtl, viscosity, density and thermal conductivity to be used for the heat transfer of airside. The sum of CO<sub>2</sub>, N<sub>2</sub> and O<sub>2</sub> ratios is **99.99%**.

Once we had calculated excess air quantity ( $\lambda$ ), we had also been able to calculate how much air will be required for 1 m<sup>3</sup> CH<sub>4</sub>.



$$\text{For } 1 \text{ m}^3 \text{ CH}_4 \rightarrow 2.78 \text{ m}^3 \text{ O}_2 + 10.45 \text{ m}^3 \text{ N}_2 = 13.23 \text{ m}^3 \text{ air is required.} \quad (3.24)$$

Heat output and efficiency are the same value with B type and C type Cu HEx appliances. Since the gas used in the tests does not change, the gas net calorimetric value is also the same. Therefore the amount of gas used does not change.

The used gas flow rate  $\dot{V}_g = 2.82 \text{ m}^3/\text{h}$

For  $2.82 \text{ m}^3/\text{h}$  test gas  $\rightarrow 37.46 \text{ m}^3/\text{h}$  fresh air is used during the test which performed under the stated operating conditions.

Table 3.37. Temperature distribution over the C type SS HEx at max load (60/80°C)

MAX 60/80°C							
Back side of heat exchanger							
Temperature (°C)							
121,1	141,3	147,6	144,3	137,8	145,6	134,6	131,1
128,1	131,3	144,2	137,5	136,9	124,7	136,5	130,8
131,1	134,6	141,1	139,8	147,1	137,7	129,9	128,1
118,8	121,3	130,2	145,1	135,6	128,8	119,2	111,1
115	123,3	127,1	125,2	131,3	122,8	119,7	114,3
105,6	109,1	121	117,7	128,1	116,5	109,5	104,3
front side of heat exchanger							

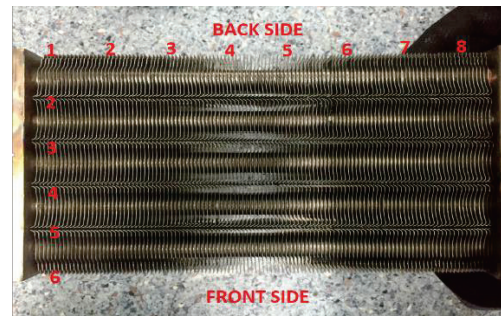


Figure 3.6. Mapping points on the SS HEx

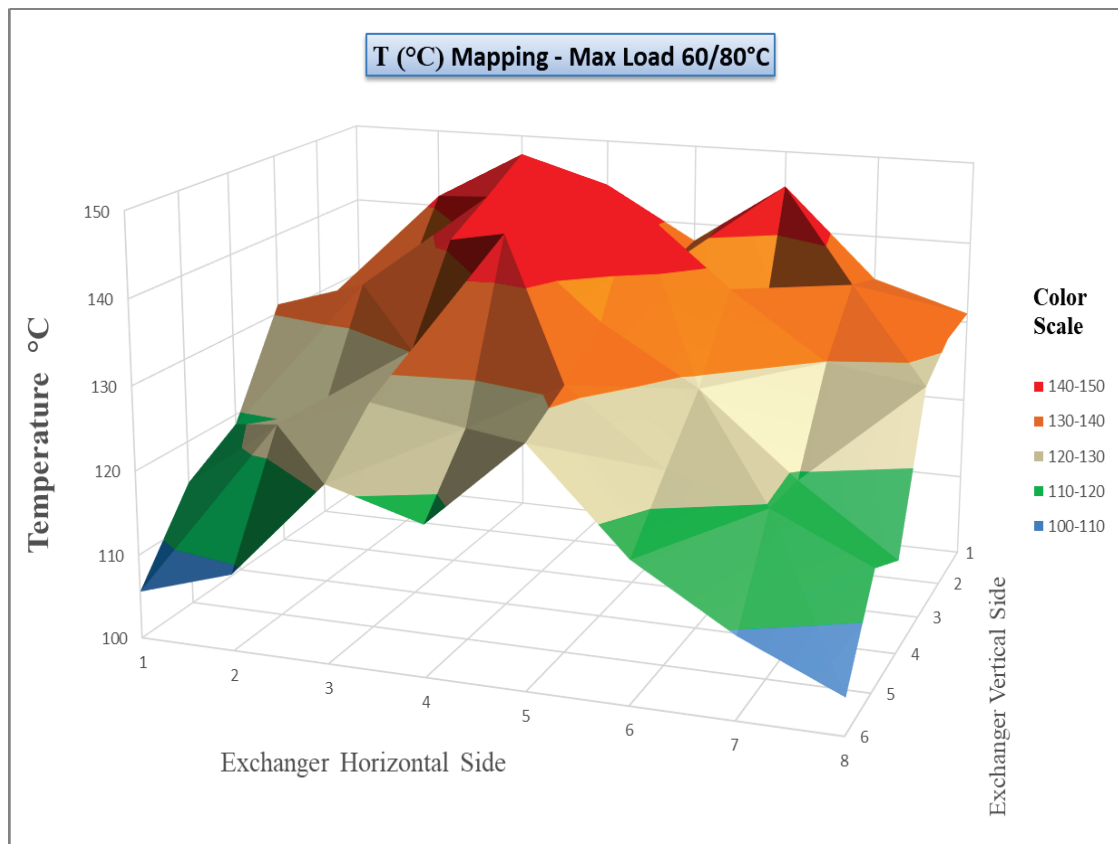


Figure 3.16. Temperature distribution over the SS HEx at max load (60/80°C) for C type appliance

Density, viscosity, Prandtl number and thermal conductivity values of CO<sub>2</sub>, N<sub>2</sub>, and O<sub>2</sub> for 357°C were taken from the thermophysical properties table<sup>5</sup> in order to calculate those values of the flue gas side.

Table 3.38. Thermophysical properties of Flue gas for the C type SS HEx at max load (60/80°C)

<b>Flue gas content (N<sub>2</sub> + CO<sub>2</sub> + O<sub>2</sub>) = 0.99</b>	0.8544	0.0817	0.063
<b>Pr<sub>fg</sub> Prandtl number of flue gas</b>	0.705		
<b>k<sub>fg</sub> Thermal conductivity of flue gas</b>	46.2×10 <sup>-3</sup>	W/m•K	
<b>ρ<sub>fg</sub> Density of flue gas</b>	0.563	kg/m <sup>3</sup>	
<b>μ<sub>fg</sub> Viscosity of flue gas</b>	3.03×10 <sup>-5</sup>	N•s/m <sup>2</sup>	

Using Equation 3.22 and 3.24 we found the gas and the fresh air flow rate to be 2.82 m<sup>3</sup>/h and 37.46 m<sup>3</sup>/h. To calculate the flue gas velocity, this value is converted to m<sup>3</sup>/s and the hydraulic diameter value for SS HEx is found and necessary calculations are made. Table 3.39 shows the calculation parameters for Re and Nu numbers.

Table 3.39. Calculation parameters and results for Re and Nu numbers and h value of Flue Gas side for the C type SS HEx at max load (60/80°C)

<b>Flue Gas Side - SS HEx</b>				
<b>Ṁ<sub>fg</sub> Gas flow rate (G20)</b>	40.3	m <sup>3</sup> /h	0.011	m <sup>3</sup> /s
<b>A<sub>fg</sub> Gas flow area</b>	0.016	m <sup>2</sup>		
<b>v<sub>g</sub> Gas velocity</b>	0.70	m/s		
<b>Dh<sub>ss</sub> Hydraulic diameter of SS HEx</b>	5.38	mm	0.00538	m
<b>Y Fin pitch</b>	2.1×10 <sup>-3</sup>	m		
<b>H Fin height</b>	0.052	m		
<b>δ<sub>f</sub> Fin thickness (t<sub>f</sub>)</b>	42×10 <sup>-5</sup>	m		
<b>Re<sub>fg</sub> Flue gas Reynolds number</b>	69.91			
<b>Nu<sub>fg</sub> Flue gas Nusselt number</b>	1.52			
<b>h<sub>fg</sub> Flue gas heat transfer coefficient</b>	13.05	W/m <sup>2</sup> •K		

To find the heat transfer coefficient for the water, the exchanger parameters in Table 3.40 were used. Due to exchanger parameters, water velocity and hydraulic diameter are calculated.

Table 3.40. Heat Exchanger Design Parameters for SS HEx

Parameters for SS HEx				
<b>L<sub>p</sub> pipe length</b>	1467.5	mm	1.4675	m
<b>D<sub>2</sub> outer diameter of pipe</b>	26.6	mm	0.0266	m
<b>D<sub>1</sub> inner diameter of pipe</b>	25.8	mm	0.0258	m
<b>r<sub>2</sub> outer pipe radius</b>	13.3	mm	0.0133	m
<b>r<sub>1</sub> inner pipe radius</b>	12.9	mm	0.0129	m
<b>t<sub>p</sub> thickness of pipe</b>	0.8	mm	0.0008	m
<b>A<sub>p</sub> pipe area</b>	522.8	mm <sup>2</sup>	0.00052	m <sup>2</sup>
<b>S<sub>p</sub> surface of pipe</b>	81.05	mm	0.081	m

For the C type SS HEx at max load (60/80°C), water thermophysical properties is used as 70°C like taken for Cu Hex appliances at max load (60/80°C).

Table 3.41. Results for Re and Nu numbers and h value of Water Side for the C type SS HEx at max load (60/80°C)

<b><math>\dot{V}_w</math> (Flow rate)</b>	18	l/min	0.0003	m <sup>3</sup> /s
<b>v<sub>w</sub> (water velocity)</b>	0.574	m/s		
<b>D<sub>h</sub> (Hydraulic diameter)</b>	0.0258	m		
<b>Re<sub>w</sub></b>	36142.04			
<b>Nu<sub>w</sub></b>	147.51			
<b>h<sub>w</sub></b>	3873.23	W/m <sup>2</sup> •K		

After these calculations, the heat transfer resistance is calculated.

Table 3.42. Heat Transfer Resistance Calculation Parameters for the C type SS HEx at max load (60/80°C)

<b>h<sub>fg</sub></b>	13.05	W/m <sup>2</sup> •K
<b>h<sub>w</sub></b>	3873.23	W/m <sup>2</sup> •K
<b>R<sub>f</sub>''</b>	0.0002	m <sup>2</sup> •K/W
<b>A<sub>pi</sub></b>	0.122	m <sup>2</sup>
<b>A<sub>po</sub></b>	0.118	m <sup>2</sup>
<b>A<sub>fin</sub></b>	2.28	m <sup>2</sup>
<b>η<sub>f</sub></b>	0.38	
<b>N</b>	115	
<b>η<sub>o</sub></b>	0.41	
<b><math>\frac{1}{U \times A} = \sum R</math></b>	0.85	K/W

Using heat transfer resistance and  $q$  which is founded before, gas temperatures can be calculated.

Table 3.43. Gas Temperature Results for the C type SS HEx at max load (60/80°C)

<b>q</b>	26.73	kW
<b>q<sub>1/48</sub></b>	556.875	W
<b>T<sub>fg</sub></b>	120	°C
<b>T<sub>cg</sub></b>	589.54	°C

The combustion gas, which is measured its CO<sub>2</sub> ratio and flue gas temperature over the HEx, passes through the 8<sup>th</sup> and 9<sup>th</sup> points of the divided heat exchanger when the water inlet side is taken as the zero points. And it is defined as the risky area for 60/80°C water cycle at max load for C type SS HEx appliance.

Table 3.44. Regional Water and Pipe Outer Surface Temperatures at Risky Area for the C type SS HEx at max load (60/80°C)

<b>T<sub>water inlet</sub></b>	60	°C
<b>T<sub>regional water 8<sup>th</sup></sub></b>	63.54	°C
<b>T<sub>regional water 9<sup>th</sup></sub></b>	63.98	°C
<b>q<sub>net1/48</sub></b>	556.875	W
<b>ΣR<sub>water to pos</sub></b>	0.0038	°C /W
<b>T<sub>regional pipe outer surface 8<sup>th</sup></sub></b>	65.22	°C
<b>T<sub>regional pipe outer surface 9<sup>th</sup></sub></b>	65.66	°C

The dew point value indicated in Table 2.3 for %8.17 CO<sub>2</sub> ratio is specified as 50.9°C. Since the pipe outer surface temperatures passing through those areas of the heat exchanger are 65.22°C and 65.66°C, and does not go below 50.9°C for 60/80°C water cycle, no condensation is observed in this region and in these operating conditions of the appliance. This was also physically controlled.

According to calculations, condensation occurrence can be observed until inlet water temperatures reach up to 46°C. When the water enters the cycle at 46°C, the temperatures of the pipe outer surfaces which contact with combustion gas are 51.2°C and 51.6°C. Since the dew point value indicated in Table 2.3 for %8.17 CO<sub>2</sub> ratio is specified as 50.9°C, condensation stops after 46°C water inlet temperature.

### 3.3. Validations

As it is found before, condensation can occurs till calculated water inlet temperatures as the limit at max load. The appliance does not work under limit water inlet temperatures in a long time period in normally, works under it for a while and reaches the target water cycle. For the purpose of seeing the occurrence of condensation, the appliance was forced to work under this condition via set the parameters on the test rig and was maintained this working parameter for a long time to see lifetime effects of condensation.

After operating the appliance for a while under condensation conditions, the front panel was unscrewed and the heat exchanger was inspected visually. During the tests, the regional condensation was observed in the area considered risky during the C type – 60/80°C max load mapping tests. This finding is shown in figure 3.17 and 3.18.



Figure 3.17. The observation of regional condensation while working the appliance under condensation conditions (C type – 60/80°C at max load)





Figure 3.18. The appearance of regional condensation on the heat exchanger (C type – 60/80°C at max load)

Soot formation which is shown in figure 3.19 and copper corrosion which is shown in figure 3.20 had been observed when the appliance runs for a long time under condensation conditions due to inlet-outlet water cycle.

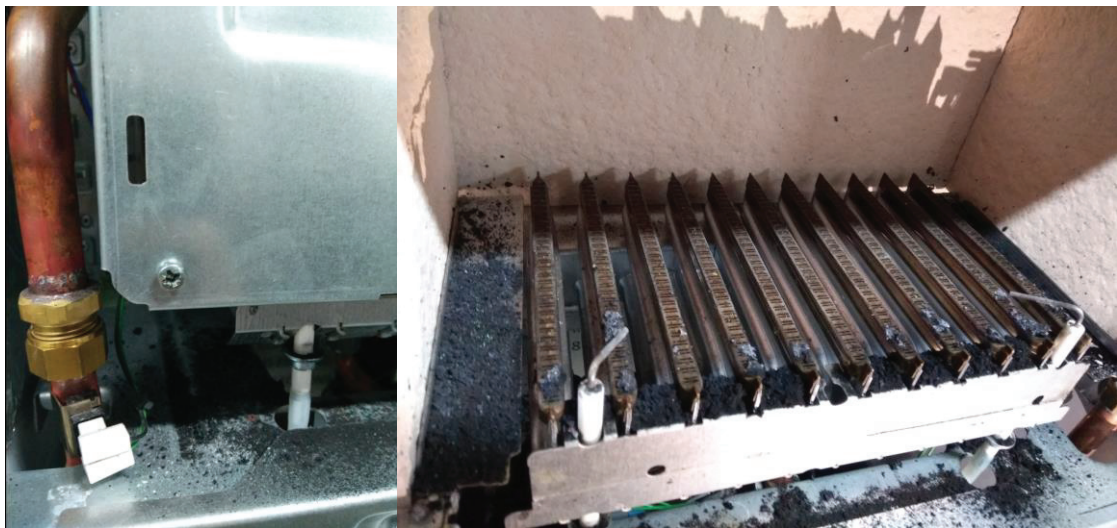


Figure 3.19. A formation of soot after running a long time in condensation conditions

Corrosion in the fins causes a decrease in the heat transfer from flue gas to the heat exchanger. Meanwhile, soot which accumulation on the burner and in the combustion chamber decreases the efficiency of the appliance by effecting flame profile and combustion.



Figure 3.20. A formation of corrosion after running a long time in condensation

Combi boiler appliance does not always work at full load. Especially in order to reach the comfort temperature at the beginning, it works at max load with  $\Delta T = 20^{\circ}\text{C}$  and tries to bring the environment to the desired temperature as soon as possible.  $\text{CO}_2$  ratios in the flue gas are high because of working at max load. For this reason, dew point temperatures rise.

For example, for the B type appliance with the copper heat exchanger, it was calculated in chapter 3, section 2 that the condensation occurs up to  $46^{\circ}\text{C}$  inlet water temperature. The inlet water temperature is assumed approximately  $15^{\circ}\text{C}$ , even if it depends on the season and area. This means that there is a condensation occurrence in the appliance until the inlet water temperature is  $46^{\circ}\text{C}$ . For avoiding from this, the appliance is operated up to a certain temperature at min load to raise the inlet water temperature. This is because the appliance has low  $\text{CO}_2$  ratios at the min load and therefore the dew point temperatures are low as well. The appliance works with the min load in the low inlet temperature values until the inlet water temperature reaches a certain level, thereafter it goes into operation in the max load mode. As the output of the study, we calculated the limit temperature the appliance should work during the minimum load operation period. With the working algorithm written according to this limit temperature, the appliance has performed a work without being exposed to condensation nearly at no point. The heat exchanger observation after performed the test is shown in figure 3.21.





Figure 3.21. The heat exchanger after the condensation tests

## CHAPTER 4

### CONCLUSION

Since there is no uniform air flow in conventional appliances, the CO<sub>2</sub> percentages and temperature distributions over the heat exchanger are not uniformly distributed. However, when considering the CO<sub>2</sub> percentages distribution for each appliance and every test condition, risky regions for condensation can change. This can be seen in the mapping test results in chapter 3, section 2.

The dew point - %CO<sub>2</sub> graph in the literature was used to find critical temperature values for condensation. The graph is presented in figure 2.13 which is in chapter 2, section 4.

In mapping tests, only the min load 47/53°C and max load 60/80°C results were shared because these test conditions had the highest CO<sub>2</sub> percentages at min load and max load. The measurement results are presented in chapter 3, section 2.

Tests made for the first case showed that the CO<sub>2</sub> percentages and temperature distributions change due to different air volumes entering the appliance which use the same heat exchanger. It is observed that the temperatures of the combustion gas below the heat exchanger were lower when the appliances had higher fresh air amount. The comparison table between B and C type is presented in Table 2.

Table 4.1. Comparison results between B type and C type appliances

47/53 °C		Parameters	60/80 °C	
Appliance Type			Appliance Type	
B Type Cu HEx	C Type Cu HEx		B Type Cu HEx	C Type Cu HEx
3	3,3	% CO <sub>2</sub>	8,87	6,1
5,21	4,57	λ	0,58	1,65
32,38	29,52	Fresh Air (m³)	34,72	49,21
66,9	70,1	Flue Gas Temperature (°C)	120	112
220,5	232,9	Combustion Gas Temperature (°C)	604	531,1
18,28	17,23	Flue Gas Heat Transfer Coefficient (W/m2•K)	17,37	21,85
0,82	0,87	Thermal Resistance (K/W)	0,87	0,75
48,75	48,45	Regional Pipe Outer Surface Temperature (°C)	67,7	63,7
		Critic Water Inlet Temperature for Condensation (°C)	46	41

As a result of calculations made by finding a heat transfer correlation for each Nusselt number that converging the results for both the air side and the water side, the critical inlet water temperatures for the condensation were found at different values for the appliances.

Tests made for the second case showed that the CO<sub>2</sub> percentages and temperature distributions change due to the heat transfer coefficient. Heat transfer coefficient changes when the fin materials and dimensions were changed. The comparison table between copper fin heat exchanger and stainless steel heat exchanger is presented in table 3.45.

Table 4.2. Comparison results between heat exchangers with Cu fin and SS fin

<b>60/80 °C</b>		
<b>C Type - Cu HEx</b>	<b>Parameters</b>	<b>C Type - SS HEx</b>
339	<b>k<sub>f</sub> (W/m<sup>2</sup>•K)</b>	25
6,1	<b>% CO<sub>2</sub></b>	8,17
1,65	<b>λ</b>	0,78
49,21	<b>Fresh Air (m<sup>3</sup>)</b>	34,46
112	<b>Flue Gas Temperature (°C)</b>	115
531,1	<b>Combustion Gas Temperature (°C)</b>	589
21,85	<b>Flue Gas Heat Transfer Coefficient (W/m<sup>2</sup>•K)</b>	13,05
0,75	<b>Thermal Resistance (K/W)</b>	0,85
63,7	<b>Regional Pipe Outer Surface Temperature (°C)</b>	65,2
41	<b>Critic Water Inlet Temperature for Condensation (°C)</b>	46

The condensation occurs especially at the beginning of the max load and 60/80C operating conditions. For avoiding from this, the preventive software is used for appliances to start them at min load.

The use of the temperature values found from the calculations will be useful at the determination of the min load operating period and this will decrease the risk of condensation on the heat exchanger.

An example of a regional condensation that may form on the exchanger if no preventing action is taken for condensation, is given in figures 3.17 and 3.18 in chapter 3 section 3. If the appliance works under that condition in a long time, the formation of the soot and corrosion can be shown in figure 3.19 and 3.20 in the same section.

If the preventions in the appliance are sufficient, the heat exchanger will be seen as in Figure 3, section 3, section 3. Using the calculation method instead of the life tests gives the same result in less time and cost.

## REFERENCES

1. *Kombi tanımı ve tipleri*. Retrieved May 2, 2018, from [https://www.alarko-carrier.com.tr/ebulten/YeniUrun/images\\_2/KombiTipleri.pdf](https://www.alarko-carrier.com.tr/ebulten/YeniUrun/images_2/KombiTipleri.pdf)
2. *Superser F150 radiant portable heater*. Retrieved May 10, 2018, from <https://www.flogas.co.uk/shop/heating/portable-gas-heaters/superser-fl50-radiant#>
3. Bosch Thermotechnology internal documents
4. *Flueing*. Retrieved May 10, 2018, from <https://www.rinnaiuk.com/hotechnology/system-design-considerations/flueing/>
5. Bergman, T. L., Lavigne, A. S., Incropera, F. P., & DeWitt, D. P. (2011). *Fundamentals of heat and mass transfer – Seventh edition*.
6. *Heat exchangers*. Retrieved May 2, 2018, from <https://classes.engineering.wustl.edu/mase-thermal-lab/me372b5.htm>
7. Thulukkanam, K. (2017). *Heat exchanger design handbook - Second edition*. ; Kakaç, S., Liu H., & Pramuanjaroenkij, A. (2012). *Heat exchangers selection, rating, and thermal design- Third edition*.
8. Frass, F. (2007). *Principles of finned-tube heat exchanger design for enhanced heat transfer - Second edition*.
9. *Finned tube heat exchanger*. Retrieved May 4, 2018, from <https://www.maxxtec.com/en/product/automatisch-aus-titel-generieren/heat-exchanger/finned-tube-heat-exchanger-maxxtec>; *A fin tube heat exchanger gives good air heat exchanger efficiency*. Retrieved May 4, 2018, from <https://www.brighthubengineering.com/hvac/63955-a-fin-tube-heat-exchanger-gives-good-air-heat-exchanger-efficiency/>
10. *Plate heat exchanger working principle*. Retrieved May 7, 2018, from <https://www.onda-it.com/eng/news/how-a-plate-heat-exchanger-works/plate-heat-exchanger-working-principle>
11. Wang, L., Sundén, B., & Manglik, R. M. (2007). *Plate heat exchangers: Design, applications and performance – First edition*.
12. Kakaç, S., & Liu H. (1997). *Heat exchangers selection, rating, and thermal design – Second edition*.
13. Wang, C. C., Fu W. L., & Chang C. T. (1997). Heat transfer and friction characteristics of typical wavy fin-and-tube heat exchangers. *Experimental Thermal and Fluid Science*, 14(2), 174-186. [https://doi.org/10.1016/S0894-1777\(96\)00056-8](https://doi.org/10.1016/S0894-1777(96)00056-8)

14. Jang, J.-Y., Wu M.-C., & Chang W.-J. (1996). Numerical and experimental studies of threedimensional plate-fin and tube heat exchangers. *International Journal of Heat and Mass Transfer*, 39(14), 3057-3066.  
[https://doi.org/10.1016/0017-9310\(95\)00341-X](https://doi.org/10.1016/0017-9310(95)00341-X)
15. Bilir L., İlken Z., & Ereğ A. (2012). Numerical optimization of a fin-tube gas to liquid heat exchanger. *International Journal of Thermal Sciences*, 52, 59-72.  
<https://doi.org/10.1016/j.ijthermalsci.2011.09.010>
16. Chang Y.-J., & Wang C.-C. (1997). A generalized heat transfer correlation for louver fin geometry. *International Journal of Heat and Mass Transfer*, 40(3), 533-544. [https://doi.org/10.1016/0017-9310\(96\)00116-0](https://doi.org/10.1016/0017-9310(96)00116-0)
17. Li P., & Norris S. (2016). Heat transfer correlations for CO<sub>2</sub> flowing condensation in a tube at low temperatures. *Applied Thermal Engineering*, 93, 872-883.  
<https://doi.org/10.1016/j.applthermaleng.2015.09.072>
18. Bilirgen H., Dunbar S., & Levy E. K. (2013). Numerical modeling of finned heat exchangers. *Applied Thermal Engineering*, 61(2), 278-288.  
<https://doi.org/10.1016/j.applthermaleng.2013.08.002>
19. Seo Y.-S., Yu S.-P., Cho S.-J., & Song K.-S. (2003). The catalytic heat exchanger using catalytic fin tubes. *Chemical Engineering Science*, 58(1), 43-53.  
[https://doi.org/10.1016/S0009-2509\(02\)00475-X](https://doi.org/10.1016/S0009-2509(02)00475-X)
20. Kaya, E., Özbaltı, N., & Altay, H. M. (2010). Preventing Boiling Problem With Computational Fluid Dynamics in Finned-Tube Special Heat Exchangers, *Mühendis ve Makina*, 51(610), 20-24. Retrieved from  
[http://www1.mmo.org.tr/resimler/dosya\\_ekler/c19921893d1da04\\_ek.pdf?dergi=1069](http://www1.mmo.org.tr/resimler/dosya_ekler/c19921893d1da04_ek.pdf?dergi=1069)
21. Wang C.-C., Lee W.-S., & Sheu W.-J. (2001). A comparative study of compact enhanced fin-and-tube heat exchangers. *International Journal of Heat and Mass Transfer*, 44(18), 3565-3573. [https://doi.org/10.1016/S0017-9310\(01\)00011-4](https://doi.org/10.1016/S0017-9310(01)00011-4)
22. Kuvannarat T., Wang C.-C., & Wongwises S. (2006). Effect of fin thickness on the air-side performance of wavy fin-and-tube heat exchangers under dehumidifying conditions. *International Journal of Heat and Mass Transfer*, 49(15–16), 2587-2596. <https://doi.org/10.1016/j.ijheatmasstransfer.2006.01.020>
23. Pirompugd W., Wang C.-C., & Wongwises S. (2009). A review on reduction method for heat and mass transfer characteristics of fin-and-tube heat exchangers under dehumidifying conditions. *International Journal of Heat and Mass Transfer*, 52(9–10), 2370-2378.  
<https://doi.org/10.1016/j.ijheatmasstransfer.2008.10.019>
24. Eldeeb R., Aute V., & Radermacher R. (2016). A survey of correlations for heat transfer and pressure drop for evaporation and condensation in plate heat exchangers. *International Journal of Refrigeration*, 65, 12-26.  
<https://doi.org/10.1016/j.ijrefrig.2015.11.013>

25. Dal, A. R. (2007). *Numerical Analysis Of The Effect On The Combi Boiler Efficiency Of Heat Exchanger Different Fin Geometries Used In The Combi Boilers* (Doctoral dissertation). Available from Council of Higher Education Thesis Center. (Thesis No: 201031)
26. Yang J., Jacobi A., & Liu W. (2017). Heat transfer correlations for single-phase flow in plate heat exchangers based on experimental data. *Applied Thermal Engineering*, 113, 1547-1557.  
<https://doi.org/10.1016/j.applthermaleng.2016.10.147>
27. Wang C.-C., & Chi K.-Y. (2000) Heat transfer and friction characteristics of plain fin-and-tube heat exchangers, part I: New experimental data. *International Journal of Heat and Mass Transfer*, 43(15), 2681-2691.  
[https://doi.org/10.1016/S0017-9310\(99\)00332-4](https://doi.org/10.1016/S0017-9310(99)00332-4)
28. Wang C.-C., Chi K.-Y., & Chang C.-J. (2000) Heat transfer and friction characteristics of plain fin-and-tube heat exchangers, part II: Correlation. *International Journal of Heat and Mass Transfer*, 43(15), 2693-2700.  
[https://doi.org/10.1016/S0017-9310\(99\)00333-6](https://doi.org/10.1016/S0017-9310(99)00333-6)
29. Karthik P., Kumaresan V., & Velraj R. (2015). Experimental and parametric studies of a louvered fin and flat tube compact heat exchanger using computational fluid dynamics. *Alexandria Engineering Journal*, 54(4), 905-915.  
<https://doi.org/10.1016/j.aej.2015.08.003>
30. Vignali G. (2017). Environmental assessment of domestic boilers: A comparison of condensing and traditional technology using life cycle assessment methodology. *Journal of Cleaner Production*, 142(4), 2493-2508.  
<https://doi.org/10.1016/j.jclepro.2016.11.025>
31. Liu X., Yu J., & Yan G. (2014). A numerical study on the air-side heat transfer of perforated finned-tube heat exchangers with large fin pitches. *International Journal of Heat and Mass Transfer*, 100, 199-207.  
<https://doi.org/10.1016/j.ijheatmasstransfer.2016.04.081>
32. Čarija Z., Franković B., Perčić M., & Čavrak M. (2014). Heat transfer analysis of fin-and-tube heat exchangers with flat and louvered fin geometries. *International Journal of Refrigeration*, 45, 160-167.  
<https://doi.org/10.1016/j.ijrefrig.2014.05.026>
33. *Combustion*. Retrieved May 11, 2018, from <https://www.britannica.com/science/combustion>
34. *Combustion definition (Chemistry)*. Retrieved May 11, 2018, from <https://www.thoughtco.com/definition-of-combustion-605841>
35. *Combustion air requirements for oil burners*. Retrieved May 11, 2018, from <https://www.beckettcorp.com/support/tech-bulletins/combustion-air-requirements-for-oil-burners/>



36. Schmidt-Rohr, K. (2015). Why combustions are always exothermic, yielding about 418 kJ per mole of O<sub>2</sub>. *Journal of Chemical Education*, 92(12), 2094-2099. doi:10.1021/acs.jchemed.5b00333
37. *Yanma nedir, ateş nasıl “yanar”?*. Retrieved May 11, 2018, from <http://www.kozmikanafor.com/yanma-nedir-ates-nasil-yanar/>
38. Atakök, G. *Kazanlar – Marmara university course note*. Retrieved from <http://mimoza.marmara.edu.tr/~gatakok/enerji/8.htm>
39. Kadirgan, N. (1991). *Doğal gazın fiziksel özellikleri, yanması, yanma ürünleri ve hava kirliliği*. Retrieved from <https://docplayer.biz.tr/21861750-Dogal-gazin-fiziksel-ozellikleri-yanmasi-yanma-urunleri-ve-hava-kirliligi-prof-dr-neset-kadirgan-y-u-muhendislik-fakultesi-dekan-yardimcisi.html>
40. Annamalai, K., & Puri I. K. (2006). *Combustion science and engineering – First edition*.
41. Kushari, A., & De, A. (2016). A short course on combustion: Fundamental and applications – Indian institute of technology Kanpur. Retrieved from <https://www.iitk.ac.in/tkic/workshop/gian/2/content/GIAN-Lecture-6.pdf>
42. Küçüka, S. *Yanma ve alev – Dokuz eylul university course notes*. Retrieved from [http://kisi.deu.edu.tr/serhan.kucuka/YANMA\\_ve\\_ALEV.pdf](http://kisi.deu.edu.tr/serhan.kucuka/YANMA_ve_ALEV.pdf)
43. Poinso, T. J., & Veynante D. P. (2004). *Theoretical and numerical combustion - Second edition*.
44. *What is the composition of air?*. Retrieved May 14, 2018, from <http://www.ency123.com/2013/08/what-is-air-made-of.html>
45. *Air - Composition and molecular weight*. Retrieved May 14, 2018, from [https://www.engineeringtoolbox.com/air-composition-d\\_212.html](https://www.engineeringtoolbox.com/air-composition-d_212.html)
46. *Combustion fundamentals*. Retrieved May 14, 2018, from <https://www.myodesie.com/wiki/index/returnEntry/id/3054>
47. *Chemical composition of natural gas*. Retrieved May 16, 2018, from <https://www.uniongas.com/about-us/about-natural-gas/chemical-composition-of-natural-gas>
48. *Methane (natural gas, biomethane)*. Retrieved May 20, 2018, from [http://www.iea-amf.org/content/fuel\\_information/methane](http://www.iea-amf.org/content/fuel_information/methane)
49. *Ramping up system performance*. Retrieved May 16, 2018, from <https://www.hpacmag.com/features/hydronics-factors-affecting-system-efficiency/>
50. İşyarlar, B., & Kırbaş, İ. (2015). Doğal gaz yakıtlı bir yanma odasında hava ve yakıt hızlarının sıcaklık, entalpi ve entropi üzerindeki etkisinin incelenmesi *GÜFBED/GUSTIJ*, 5(2), 60-66. <http://dx.doi.org/10.17714/gufbed.2015.05.005>